Hybrid Control of a Pneumatic Artificial Muscle (PAM) Robot Arm Using an Inverse NARX Fuzzy Model

Ho Pham Huy Anh[2] and Kyoung Kwan Ahn[1*]

[1] School of Mechanical and Automotive Engineering, University of Ulsan, Ulsan, Korea

*Corresponding Author (Tel : +82-52-259-2282; E-mail: kkahn@ulsan.ac.kr)

[2] Faculty of Electrical and Electronic Engineering, Ho Chi Minh City University of Technology, Viet Nam (Tel : +84-908229736; E-mail: hphanh@hcmut.edu.vn)

Abstract

We investigated the possibility of applying a hybrid feed-forward inverse nonlinear auto-regressive with exogenous input (NARX) fuzzy model-PID controller to a nonlinear pneumatic artificial muscle (PAM) robot arm to improve its joint angle position output performance. The proposed hybrid inverse NARX fuzzy-PID controller is implemented to control a PAM robot arm that is subjected to nonlinear systematic features and load variations in real time. First the inverse NARX fuzzy model is modeled and identified by a modified genetic algorithm (MGA) based on input/output training data gathered experimentally from the PAM system. Second the performance of the optimized inverse NARX fuzzy model is experimentally demonstrated in a novel hybrid inverse NARX fuzzy-PID position controller of the PAM robot arm. The results of these experiments demonstrate the feasibility and benefits of the proposed control approach compared to traditional PID control strategies. Consequently the good performance of the MGA-based inverse NARX fuzzy model in the proposed hybrid inverse NARX fuzzy-PID position control of the PAM robot arm is demonstrated. These results are also applied to model and to control other highly nonlinear systems.

***Keywords*:** modeling and identification, nonlinear inverse NARX fuzzy model, pneumatic artificial muscle (PAM) robot arm, modified genetic algorithm (MGA) optimization, hybrid inverse NARX fuzzy-PID control.

1. INTRODUCTION

A new type of pneumatic actuator, the pneumatic artificial muscle (PAM), is becoming increasingly popular for used in precision robotic tasks as well as in human exoskeleton technologies intended to enhance strength and mobility. PAM possesses all the advantages of traditional pneumatic actuator (i.e., low cost, light weight) along with high power/weight and power/volume ratios (Chou *et al.*, 1994a). This is an advantage for robotic and exoskeleton applications in which heavy actuators can add significantly to the payload (Chou *et al.*, 1994b; Tsagarakis *et al.*, 2000; Caldwell *et al.*, 1995; Cocatre-Zilgien *et al.*, 1996; Pack *et al.*, 1997; Ahn and Anh, 2006, 2007a; Ahn and Thanh, 2006).

A major problem inherent to PAM actuators and to pneumatic actuators in general, is the problem of precise control. This problem occurs because pneumatic actuators are highly nonlinear and their properties vary with time. Since rubber tube and plastic sheath components are continually in contact with each other and its shape is continually changing, the PAM's temperature fluctuates and changes the properties of the actuator over time. Approaches to PAM control have included PID control, adaptive control (Lilly, 2003), nonlinear optimal predictive control (Reynolds *et al.*, 2003), variable structure control (Repperger *et al.*, 1998; Medrano-Cerda *et al.*,1995), gain scheduling (Repperger *et al.*,1999), and various soft computing approaches including neural network Kohonen training algorithm control (Hesselroth *et al.*,1994), neural network + nonlinear PID controller (Ahn and Thanh, 2005), and neuro-fuzzy/genetic control (Chan *et al.*, 2003; Lilly *et al.*, 2003).

Due to their highly nonlinear nature and time-varying parameters, PAM robot arms present a challenging nonlinear model problem. Previous studies have used a number of approaches to model PAM actuators. Balasubramanian *et al.*, (2003a) applied the fuzzy model to identify the dynamic characteristics of PAM and later applied the nonlinear fuzzy model to model and to control of the PAM system. Lilly (2003) presented a direct continuous-time adaptive control technique and applied it to control joint angle in a single-joint arm. Tsagarakis *et al.* (2000) developed an improved model for PAM. The disadvantage of these PAM manipulator models lies in their mathematical approaches, which are too complex to apply in practice. Hesselroth *et al.* (1994) presented a neural network that controlled a five-link robot using back propagation to learn the correct control over a period of time. Repperger *et al.* (1999) applied a gain scheduling model-based controller to a single vertically hanging PAM. Chan *et al.*, (2003) and Lilly *et al.*, (2003) introduced a fuzzy P+ID controller and an evolutionary fuzzy controller, respectively, for the PAM system. The novel feature is a new method of identifying fuzzy models from experimental data using evolutionary techniques. Unfortunately, these fuzzy models are clumsy and have only been tested in simulation studies. Previously, we (Ahn and Anh,

2006) applied a modified genetic algorithm (MGA) for optimizing the parameters of a linear ARX model of the PAM manipulator which can be modified online with an adaptive self-tuning control algorithm, and then (Ahn and Anh, 2007b) successfully applied recurrent neural networks (RNN) for optimizing the parameters of neural NARX model of the PAM robot arm. Recently, we (Ahn and Anh, 2009) successfully applied the modified genetic algorithm (MGA) for optimizing the parameters of the NARX fuzzy model of the PAM robot arm.

The implementation of a simple but efficient model for the one-link PAM robot arm that can not only be utilized efficiently for modeling, identification and simulation but also can be applied efficiently to the control of highly nonlinear systems like the PAM robot arm remains a challenging problem. Conventionally, the fuzzy models based on expert human knowledge of the system were used for such problems and often involved heuristic trial and error approach. Recently, research has been conducted to tune fuzzy models using real data (Nelles O., 2000). Real data would make it possible to develop a good fuzzy model of a system while restricting the complexity of the model. For the purposes of nonlinear system control, a fuzzy model obtained from the experimental input-output training data set is required for prediction, simulation, optimization and control of an unknown system plant.

In this paper we describe the modeling and identification of a PAM robot arm actuated by a group of antagonistic PAM pairs. We suggest a modified genetic algorithm (MGA) for the generation of an inverse NARX fuzzy model (INFM) based on the experimental input-output data obtained from a PAM robot arm system. In this way, the proposed MGA algorithm optimally generates appropriate fuzzy if-then rules to characterize the dynamic features of the PAM robot arm. The proposed INFM model identification approach based on the MGA method is successfully applied to control not only the PAM robot arm system but also other dynamic nonlinear processes.

The unique contributions of this paper include the fact that for the first time, the modeling and identification of the proposed inverse NARX fuzzy model of the PAM robot arm are realized; the optimization of the inverse NARX fuzzy model's parameters of the PAM robot arm is completed using an MGA; an efficient inverse NARX fuzzy model is formulated in both first order NARX11 and second order NARX22 structures and shown to be suitable for the control of highly nonlinear PAM robot arm; and finally the good performance of the MGA-based inverse NARX fuzzy model in the proposed hybrid inverse NARX fuzzy-PID position control of the PAM robot arm is demonstrated.

The paper is arranged as follows. Section 1 is a literature review highlighting studies addressing the modeling and identification of PAM robot arms, and presents novel features of MGA-based identification using the inverse NARX fuzzy model investigated in this paper. Section 2 introduces the proposed modified genetic algorithm (MGA) used for PAM robot arm modeling and identification.

Section 3 presents the INFM model. Section 4 presents the hardware configuration of the PAM robot arm and introduces the proposed hybrid inverse NARX fuzzy-PID control of the PAM robot arm. Section 5 presents and analyzes the results of MGA-based modeling and identification of the inverse NARX fuzzy model and assesses its performance in the proposed hybrid inverse NARX fuzzy-PID control scheme. Section 6 concludes the paper.

2. MODIFIED GENETIC ALGORITHM (MGA) FOR IDENTIFYING THE INVERSE NARX FUZZY MODEL

Classic genetic algorithm (GA) involves three basic operations: reproduction, crossover and mutation. To derive a solution to a near optimal problem, GA creates sequences of populations that correspond to the numerical values of a particular variable. Each individual, namely a chromosome, in a population represents a potential solution to the problem in question. Selection is the process by which chromosomes in a population that contain better fitness value have a greater probability of reproducing. In this paper, we used a roulette-wheel selection scheme. Through selection, chromosomes encoded with better fitness values are chosen for recombination to yield off-springs for successive generations. Then the natural evolution (including crossover and mutation) of the population will be continued until a desired termination or error criterion is achieved. This results in a final generation containing highly fit chromosomes representing optimal solutions to the searching problems. Figure 1 describes the procedure of GA optimization.

2.1. Modifications to the conventional genetic algorithm

In recent years, considerable research has focused on improving GA performance (Chen *et al.*, 2000; Potts *et al.*, 1994; Back *et al.*, 2001). Inappropriate choices of operators and parameters used in the GA process make GAs susceptible to premature convergence. In this paper, an attempt is made to simultaneously apply the proposed improved strategies to overcome such problems.

(1) *Extinction strategy*:

Because of the properties of global optimization and the fast convergence of the GA process, after a certain number of generations, the searching process thus tends to stagnate and the final result may be trapped into a local optimum. The only mechanism of the conventional GA that generates better chromosomes is mutation. Unfortunately, slow mutation rates must be chosen to yield a stable process. These slow rates lead to very small increases in fitness values especially for long chromosomes. This paper introduces a novel technique called the extinction strategy to overcome this problem. Based on this concept, if no further increases in the fitness value are detected; i.e., a variance equal to zero, the best $q\%$ of chromosomes survive every L_e generation according to their

better fitness values. The others are randomly generated to fill out the population. The surviving chromosomes are allowed to mate as usual to form the next generation.

(2) *Elitist strategy*:

When creating a new population by crossover and mutation, the best chromosomes may be lost. The elitist strategy guarantees the survival of the best individual in a generation. Thus, this strategy ensures the continuous increase of maximum fitness values from generation to generation. Practically, this strategy can be implemented by replacing the worst chromosome in the next generation with the best chromosome of the previous generation. Consequently, elitism can rapidly increase the performance of the GA.

(3) *G-bit strategy*:

A single bit mutation of a chromosome can be thought of as a local search in an area surrounding that chromosome within a multi-dimensional space. When the population converges prematurely to a local optimum, a single bit mutation may be required to relocate to a new region. A high mutation rate proves helpful in this situation, but it may also tend to transform the genetic search into a random search. To solve this problem, this paper will apply an extra operation, called the G-bit operation, to the GA process. Back *et al.* (2001) introduced G-bit improvement as a simply change of a single bit value from 0 to 1 or vice versa if the fitness of this modified string is better than that of the original string. Otherwise the original string remains unchanged. This test is executed repeatedly from the first bit to the last bit of a string. Furthermore, in order to save computing time, the G-bit improvement is only applied to the best individual in a generation.

In this paper, the proposed MGA adopts all of these advanced strategies. The elitist strategy and G-bit operation ensures a steady increase of the maximum fitness value. The extinction strategy prevents the searching process from being trapped in a local optimum. Consequently, the overall efficiency and the searching process of the optimum solution are improved by these modifications.

2.2. Modified genetic algorithm (MGA) for optimizing inverse NARX fuzzy model's parameters

A general nonlinear model is considered:

$$y(k) = f(W, Y, U) \tag{1}$$

where $f()$ is a nonlinear function such that (1) is stable; $W = [w_1, w_2, .., w_h]$ is a set of h fixed parameters; $Y = [y(k-1), .., y(k-n)]$ is a set of n autoregressive output terms and $U = [u(k-1), .., u(k-m)]$ is a set of m past input values.

In the case that the structure of $f(.)$ is assumed to be known, Equation (1) can be estimated as

$$\hat{y}(k) = f(\hat{W}, Y, U) \tag{2}$$

where $\hat{W} = [\hat{w}_1, ..., \hat{w}_h]$ is a set of h parameters estimated and $\hat{y}(k)$ is the estimated output.

In order to apply the novel proposed MGA, each estimated parameter $\hat{w}_i$ (i=1,$\cdots$, h) will be encoded as a binary string called a gene. All genes are cascaded to form a longer string $\hat{W}$ called a chromosome. This MGA-based identification strategy is used to search for the best chromosome $\hat{W}$ so that $\hat{y}(k) \to y(k)$ from the testing input-output data range. Each generation will explore a collection of N chromosomes of estimated parameters.

Consider the fitness value F_j associated with the j^{th} chromosome in a population that is defined as

$$F_j = 10^4.(\frac{1}{M}\sum_{k=1}^{M}(y(k) - \hat{y}_j(k))^2)^{-1} \tag{3}$$

in which k is the discrete time index in the identification process; M is the window size through which errors will be accumulated and $\hat{y}_j(k)$ is the estimated k^{th} output that belongs to the j^{th} chromosome of the estimated parameters. In each generation, the MGA will search for the maximum fitness value over the entire space of parameters. Experimentally, the larger the M value is when modified, the slower the execution of the MGA becomes. Unfortunately, a small M value tends to cause the estimation to oscillate. Consequently, a trade-off should be considered when choosing an available M value.

Before running the MGA algorithm, it needs to tune the following parameters:

P_c: crossover rate used in the crossover operation

P_m: mutation rate used in the mutation operation

D: number of chromosomes chosen for mating as parents used in the crossover operation

N: number of chromosomes in each generation

L_t: number of generations tolerated for no improvement on the value of the fitness before the MGA is terminated

L_e: number of generations tolerated for no improvement on the value of the fitness before the operator extinction is applied. It needs to pay attention that $L_e \langle\langle L_t$.

ρ: portion of the chosen parents permitted to survive into the next generation used in the crossover operation

q: percentage of chromosomes survived according to their fitness values in the extinction strategy

The steps of the MGA-based model identification procedure are summarized as follows:

Step 1: tune the parameters as described above. Encode the estimated parameters into genes and chromosomes as a string of binary digits. Considering that the parameters lie in several bounded regions η_k

$$|w_k| \le \eta_k \qquad \text{for } k=1,\ldots,h. \tag{4}$$

The length of the chromosome needed to encode W_k is based on η_k and the desired accuracy δ_k. Set $i = k = m = 0$.

Step 2: Randomly generate randomly the initial generation of N chromosomes. Set $i=i+1$.

Step 3: Decode the chromosomes then calculate the fitness value for every chromosome of the population in the generation. Consider $F^i_{\max}$ as the maximum fitness value in the i^{th} generation.

Step 4: Apply the elitist strategies to guarantee the survival of the best chromosome in each generation. Then apply the G-bit strategy to this chromosome to improve the efficiency of the MGA in local search.

Step 5: Combine the basic sub-steps of the conventional GA optimization

(1) *Reproduction:* In this paper, reproduction is set as a linear search through roulette wheel values weighted proportional to the fitness value of the individual chromosome. Each chromosome is reproduced with the probability of $\frac{F_j}{\sum_{j=1}^{N} F_j}$ with j being the index of the chromosome ($j=1,\ldots,N$).

(2) *Crossover:* Choose D chromosomes possessing maximum fitness values among N chromosomes of the present gene pool for mating and then allow some of them, called the ρ best chromosomes, are allowed to survive into the next generation. Parents chosen from D chromosomes will be mating with the crossover rate P_c.

(3) *Mutation:* Mutate a bit of the string ($0 \leftrightarrow 1$) with the mutation rate P_m.

Step 6: If $F^i_{\max} = F^{i-1}_{\max}$, then $k=k+1$, $m=m+1$; otherwise, $k=0$ and $m=0$.

Step 7: If $k=L_e$, then apply the extinction strategy and then set $k=0$.

Step 8: If $m=L_t$, then terminate the MGA algorithm; otherwise go to **Step 3** to run the $(i+1)^{\text{th}}$ generation.

The flow chart of the proposed MGA-based optimization and identification process of the PAM manipulator fuzzy model is given in Fig. 2.

The present research has multiple goals. First the proposed MGA will be applied to identify the PAM robot arm inverse NARX fuzzy model. Second we will compare the performance results of the proposed MGA-based inverse NARX11 fuzzy model with the proposed MGA-based inverse NARX22

fuzzy models. Finally we evaluate the performance of the proposed MGA-based inverse NARX fuzzy model in a hybrid inverse NARX fuzzy-PID position control scheme applied to a highly nonlinear PAM robot arm.

3. DESIGN AND IMPLEMENTATION OF THE MGA-BASED INVERSE NARX FUZZY MODEL

3.1. Assumptions and constraints

As the PAM robot arm system is operated nearly symmetrically, it is assumed that the symmetrical membership functions about the y-axis will provide a valid fuzzy model. A symmetrical rule-base is also assumed. The following constraints are introduced to the design of the inverse NARX fuzzy Model (INFM). First, all universes of discourses are normalized to lie between –1 and 1 with scaling factors external to the INFM used to give appropriate values to the input and output variables. Second, it is assumed that the first and last membership functions have their apexes at –1 and 1, respectively, and that only triangular membership functions are to be used. Third, the number of fuzzy sets is constrained to be an odd integer greater than unity. Finally, the base vertices of the membership functions are coincident with the apex of the adjacent membership functions. This ensures the value of any input variable is a member of at most two fuzzy sets.

3.2. Spacing parameter

The spacing parameter specifies how the centers are spaced out across the universe of discourse. This method of designing the membership functions is inspired by previous studies (Park *et al.*, 1995; Cheong *et al*., 2000). A value of one indicates even spacing, while a value smaller than unity indicates that the membership functions are more spaced out in the center of the range and closer together at the extremes as shown in Fig.3. The position of each center is calculated by taking the position where the centre would be if the spacing were even and raising this to the power of the spacing parameter. Figure 3 presents the triangle input membership function with MFs = 7 and a spacing factor = 2.

3.3. Designing the rule base

As well as specifying the membership functions, the rule-base must also be designed. To specify a rule base, characteristic spacing parameters for each variable and a characteristic angle for each output variable are used.

In the proposed construction method, certain characteristics of the rule-base are that extreme outputs usually occur when the inputs have extreme values while mid-range outputs are generated when the input values are mid-range and similar combinations of input linguistic values lead to similar output values. Using these assumptions the output space is partitioned into different regions corresponding to different output linguistic values. The space partitioning is determined by the characteristic spacing parameters and the characteristic angles. The angles determine the slope of line through the origin on which seed points are placed. The positioning of the seed points is determined by a spacing method similar to the one used to determine the center of the membership function.

Grid points representing each possible combination of the input linguistic values are also placed in the output space. These are spaced in the manner described above. The rule-base is determined by calculating which seed-point is closest to each grid point. The output linguistic value representing the seed-point is set as the consequent of the antecedent represented by the grid point. This is illustrated in Fig. 4a, which is a graph showing seed points (blue circles) and grid-points (red circles). Figure 4b shows the derived rule-base. The lines on the graph delineate the different regions corresponding to different consequents. The parameters for this example are 0.9 for both input spacing parameters, 1 for the output spacing parameter, and 45° for the angle theta parameter.

3.4. Fuzzy inference system (FIS) implementation for the inverse NARX fuzzy model.

To automatically implement the fuzzy inference system (FIS) structure for the proposed MGA-based INFM model, a necessary program is written in M-function that utilizes the fuzzy logic toolbox (FLT) for MATLAB to create the FIS. It respectively creates the membership functions and the rule-base and then creates the FIS from both of them.

First, error checking is performed to ensure that the parameters chosen by the MGA are valid. Secondly, the input/output parameters of the INFM model are called to create the membership functions of each of the input/output variables. Then creating a rule-matrix in the format required by the FLT creates a suitable rule-base for each of the output variables and puts them together in a suitable way to create the FIS. In this paper, only triangular membership functions (MF) are used. From two parameters, namely, the number of MF and the spacing parameters, the centers of each membership function are calculated. As the base vertices are at the same positions as the centers of the adjacent MFs, the calculating task of the full set of input-output MF parameters is then completed.

The next step of the FIS implementation is to create the rule-base. This step returns a rule-base based on the parameters that are passed in. These parameters are composed of a number of MFs per variable,

spacing parameters for each variable and characteristic angles for the seed lines. First, the coordinates of the seed points are calculated and then the grid-point coordinates are calculated. The consequents for each rule are then generated for each grid-point by measuring the distance to each seed point and finding the shortest one. The antecedents and consequents are then returned in a matrix in the format required by the FLT.

With all of these, a full dynamic FIS can be generated using only a number of conformable parameters. This is ideal for applying the MGA to find an optimal INFM as the MGA can work on these parameters and improve the performance of the INFM characteristics. How this is achieved is demonstrated in the next subsection.

3.5. Parameter encoding

To run an MGA, suitable encoding and bounds for each of the parameters need to be carefully decided. For this task the parameters given in Table 1 are used with the shown ranges and precisions. Binary encoding is used as necessary to allow the MGA to more flexibly search for the solution space. The numbers of the membership functions are limited to the odd integers inclusive between (3–5) in the case MGA-based PAM robot arm INFM model design. Experimentally, this was considered a reasonable constraint. The advantage of using this constraint is that this parameter can be captured in just one bit per variable.

For the spacing parameters, two separate parameters are used. The first, within the range (0.1– 1), determines the magnitude, and the second, which takes only the values –1 or 1, is the power by which the magnitude is raised. This determines whether the membership functions compress in the center or at the extremes. Consequently, each spacing parameter obtains the range (0.1 – 10). The precision required for the magnitude is 0.01, meaning that eight total bits are used for each spacing parameter.

The scaling for the input variables is allowed to vary in the range (0 – 100) while that of the output variable is given the range (0 – 1000). These values were identified after a few trials of the MGA used wider ranges, as the values returned were found to lie within these ranges. For this encoding scheme the total number of bits per chromosome are 105, 102 and up to 175 in the case of the MGA-based PAM robot arm inverse TS fuzzy model, the inverse NARX11 fuzzy model, and the inverse NARX22 fuzzy model, respectively. This means that there are 2^{102} or approximately $5x10^{30}$ potential solutions, an unknown but likely very small fraction of which represents a desirable INFM model that would be discovered by the proposed MGA. Based on the experiment results, the proposed MGA succeeds in

finding close to optimal solutions in large spaces despite having no prior knowledge. This demonstrates the power of proposed MGA.

3.6. Nonlinear inverse NARX fuzzy models for PAM robot arm.

The newly proposed INFM for a PAM robot arm presented in this paper is improved by combining the extraordinary predictive and adaptive features of the NARX model structure. The resulting model established a nonlinear relationship between the past inputs and outputs and the predicted output, where the system's prediction output is a combination of the system output produced by real inputs and the system's historical behaviors. It can be expressed as:

$$\hat{y}(k) = f\left(y(k-1),...,y(k-n_a),u(k-n_d),...,u(k-n_b-n_d)\right) \tag{5}$$

Here, n_a and n_b are the maximum lag considered for the output and input terms, respectively, n_d is the discrete dead time, and f represents the mapping of the fuzzy model.

The structure of the newly designed INFM is governed by the fact that this NARX fuzzy model interpolates between local linear, time-invariant (LTI) ARX models as follows:

Rule j: if $z_1(k)$ *is* $A_{1,j}$ *and … and* $z_n(k)$ *is* $A_{n,j}$ then

$$\hat{y}(k) = \sum_{i=1}^{n_a} a_i^j y(k-i) + \sum_{i=1}^{n_b} b_i^j u(k-i-n_d) + c^j \tag{6}$$

where the element of the $\boldsymbol{z}(k)$ "*scheduling vector*" are usually a subset of the $\boldsymbol{x}(k)$ regressors that contain the variables relevant to the nonlinear behaviors of the system,

$$Z(k) \in \{y(k-1),...,y(k-n_a),u(k-n_d),...,u(k-n_b-n_d)\} \tag{7}$$

while the $f_j(q(k))$ consequent function contains all the regressor $q(k)=[X(k)\ 1]$,

$$f_j(q(k)) = \sum_{i=1}^{n_a} a_i^j y(k-i) + \sum_{i=1}^{n_b} b_i^j u(k-i-n_d) + c^j \tag{8}$$

In the simplest case, the NARX type zero-order TS fuzzy model (the singleton or Sugeno fuzzy model which is not applied in this paper) is formulated by the simple rules consequents as:

Rule j : if $Z_1(k)$ *is* $A_{1,j}$ *and…and* $Z_n(k)$ *is* $A_{n,j}$ then

$$\hat{y}(k) = c^j \tag{9}$$

where $z(k)$ contains all inputs of the NARX model:

$$Z(k) = X(k) = \{y(k-1),...,y(k-n_a),u(k-n_d),...,u(k-n_b-n_d)\} \tag{10}$$

Thus the difference between the NARX TS fuzzy model and the fuzzy TS model method is that the output from the TS fuzzy model is linear and constant, and the output from NARX fuzzy model is the NARX function. However they have the same fuzzy inference structure (FIS).

The block diagrams presented in Fig. 5a and Fig. 5b illustrate the difference between the MGA-based PAM robot arm inverse TS fuzzy model identification and the MGA-based PAM robot arm INFM design.

The block diagrams presented in Fig. 5b and Fig. 5c illustrate the improvement from the MGA-based PAM robot arm inverse NARX11 fuzzy model identification to the MGA-based PAM robot arm inverse NARX22 fuzzy model identification. All such block diagrams will be studied thoroughly in this paper.

4. CONTROL SYSTEM AND HARDWARE CONFIGURATION SETUP

4.1. Hybrid feed-forward inverse NARX fuzzy model –PID control scheme

The novel proposed hybrid inverse NARX fuzzy-PID control scheme is depicted in the Fig. 6. Since the combination of the feedforward control and the feedback PID control in a closed–loop system is an efficient technique and has been proven to be more stable, more robust and more accurate than non-hybrid schemes (Boerlage *et al*., 2003), this hybrid scheme is used in this paper. In a feed-forward controller design, the proposed INFM of the PAM robot arm is designed offline to approximate as closely as possible the dynamic and nonlinear features of the PAM robot arm. This INFM is then incorporated in parallel with the closed–loop feedback PID controller to increase the accuracy and to ameliorate the performance of the joint position control of the PAM system. The block diagram of the proposed hybrid inverse NARX fuzzy-PID controller is shown in Fig.6.

The basic concept underlying this approach is to learn the PAM robot arm's inverse characteristics and to use the INFM to generate the compensated control signal U_{FUZZY}. The main equation of the proposed control algorithm is given by:

$$U = U_{PID} + U_{FUZZY} \tag{11}$$

where U is the required control voltage, U_{PID} is the control voltage generated by the PID controller and U_{FUZZY} is the control voltage generated by the INFM. The INFM obtains the dynamic inverse PAM manipulator model. The error $e(k)$ creates the compensating value U_{PID} through the PID controller while the proposed hybrid inverse NARX fuzzy-PID control is in operation. This occurs to compensate for modeling errors and un-modeled disturbances. Likewise, the parallel-connected conventional PID controller also contributes to a faster and more accurate tracking performance.

4.2. Experimental Setup

The prototype PAM robot arm used in this paper has two axes, is closed loop activated with two antagonistic PAM pairs, and is pneumatically driven controlled through two proportional valves. Each

of the two axes provides a different motion and contributes one degree of freedom link of the PAM robot arm (see Fig. 8).

In this paper, the first joint of the PAM robot arm is fixed and the proposed control algorithm is applied to control the joint angle position of the second joint of the PAM robot arm.

The experimental system is illustrated in Fig.9. We used a proportional valve manufactured by FESTO Corporation. An angle encoder sensor is used to measure the output angle of the joint. The entire system is a closed loop system operated through a computer. It first generates $u_0(t)$=5[v] to inflate the artificial muscles with air pressure at P_0 (initial pressure) to render the joint initial status. By changing the input $u(t)$ from the D/A converter, it could set the air pressures of the two artificial muscles at $(P_0 + \Delta P)$ and $(P_0 - \Delta P)$, respectively. As a result, the joint is forced to a certain angle and we can then measure the joint angle rotation through the rotary encoder and the counter.

The experimental apparatus is shown in Fig.10. The hardware includes an IBM compatible PC (Pentium 1.7 GHz) that sends the control voltage signal $u(t)$ to control the proportional valve (FESTO, MPYE-5-1/8HF-710B) through a D/A board (ADVANTECH, PCI 1720 card) that changes the digital signal from the PC to analog voltage $u(t)$. The torque is generated by the contraction and the dilation of the antagonistic artificial muscles. Consequently, the second joint of the PAM manipulator is rotated. The joint angle, θ[deg], is detected by a rotary encoder (METRONIX, H40-8-3600ZO) with a resolution of 0.1[deg] and fed back to the computer through a 32-bit counter board (COMPUTING MEASUREMENT, PCI QUAD-4 card), which changes digital pulse signals to a joint angle value $y(t)$. The external inertia load could be tested with two different loads (0.5[kg] and 2[kg]). The experiments are conducted under the pressure of 4[bar] and all control software is coded in MATLAB-SIMULINK with the C-mex S-function.

5. EXPERIMENTAL RESULTS.

5.1. Results of the MGA-based INFM identification of the PAM robot arm.

A prototype PAM robot arm is chosen for INFM design. The essential procedure consists of four basic steps as considered in Fig.3. The first step obtains the experimental data that describes the underlying intrinsic features of the PAM robot arm. Fig.11 presents the testing input applied to the tested PAM robot arm and the responding joint angle output collected from it. This experimental input-output data is used for training and validating the proposed INFM.

Pseudo Random Binary Signal (PRBS) input during the first 40 seconds and output from the corresponding PAM robot arm joint angle are used for estimating, while the PRBS input during the consecutive 40 seconds along with the output from the corresponding PAM robot arm joint angle will be used to validate the derived model (Fig.11).

Two different identification cases were considered, including the proposed MGA-based PAM robot arm inverse NARX11 fuzzy model and the inverse NARX22 fuzzy model.

The identification block diagram based on the experimental input-output data values measured from the PAM robot arm is shown in Fig.5. Table 1 contains the fuzzy model parameters used for encoding the optimized input values of the MGA-based optimization algorithm. The range (3–5) corresponds to the number of membership functions permitting two different odd values that would be chosen by the MGA (3 and 5).

The novel feature of the proposed inverse NARX11 fuzzy model lies in the exploitation of two input variables *Y(z)* and *U(z-1)* instead of *Y(z)* and *Ydot(z)* which are used in the conventional TS Fuzzy model. Likewise, the proposed inverse NARX22 fuzzy model is composed of four input variables *Y(z), Y(z-1), U(z-1)* and *U(z-2).* This novel structure combines the extraordinary approximating ability of the fuzzy system with the powerful predictive potentiality of the recurrent NARX structure realized in the inverse NARX11 and inverse NARX22 fuzzy models.

The convergence of the fitness values calculated based on the MGA shown in Equation (3) is presented in Fig. 12 in the case of the inverse NARX11 fuzzy model and in Fig. 14 in the case of the inverse NARX22 fuzzy model (with population = 20, P_c=0.5, P_M=0.1 and generation = 100). Both figures show that the best fitness values obtained are 168800 in the case of the inverse NARX11 fuzzy model and 186042 in the case of the inverse NARX22 fuzzy model with high speed of convergence. The best fitness value is obtained at generation 92 with the inverse NARX11 fuzzy model and generation 68 with the inverse NARX22 fuzzy model. Furthermore, the powerful ability of MGA searching enhanced by the elitism strategy, extinction strategy, and G-bit method, leads to a very good fitness value ($\approx$50000 with the inverse NARX11 and $\approx$55000 with the inverse NARX22 fuzzy model).

Consequently, the resulting inverse NARX11 and inverse NARX22 fuzzy models cover most of nonlinear features of the PAM robot arm implied in the input signals *U(z-1)*[v] and *Y(z)* [deg], and the output signal *U(z)*[v]. The estimated results of the identified PAM robot arm inverse NARX11 and inverse NARX22 fuzzy models presented in Fig.13a and Fig.15a respectively yield an excellent range of error ($<\pm$ 0.3[V] with the inverse NARX11 fuzzy model and $<\pm$ 0.15[V] with the inverse NARX22 fuzzy model). Likewise, the validation results of the MGA-based identified PAM robot arm inverse NARX11 and inverse NARX22 fuzzy models presented in Fig.13b and Fig.15b, respectively, also

show a good range of error ($< \pm 0.3$[V] with the inverse NARX11 fuzzy model and $< \pm 0.15$[V] with the inverse NARX22 fuzzy model).

These results assert the powerful potential of the proposed INFM not only for modeling and identification but also for control.

Figures 13c and Fig. 15c illustrate the shapes of the input and output membership functions and the rule-base surf-view of the proposed inverse NARX11 and inverse NARX22 fuzzy models, respectively. These two figures show that although the MGA-based NARX11 fuzzy model only requires a modest FIS structure with the MF of two inputs *U(z-1)*[v] and *Y(z)*[deg] and the output *U(z)*[V] only equal to [5, 5, 5], the shape of the surf-viewer of the proposed inverse NARX11 fuzzy model (shown in Fig. 13c) is sophisticated because the inverse NARX11 fuzzy model is capable of learning all of the dynamic features of the PAM robot arm. Likewise, Fig. 15c shows that although the MGA-based inverse NARX22 fuzzy model requires only a simple FIS structure with a membership function (MF) of four inputs (*Y(z)*[deg], *Y(z-1)*[deg], *U(z-1)* [V], *U(z-2)*[V]) and output *U(z)*[V] only equal to [3, 3, 3, 5, 5], the shape of the surf-viewer of the MGA-based inverse NARX22 fuzzy model (shown in Fig. 15d) is sophisticated and is implied on three principal surf-viewers among the total six, which confirms that it is possible for the proposed inverse NARX22 fuzzy model to learn all of the nonlinear features of the PAM robot arm contained in the input and output training signals.

These results indicate that the INFM is capable of learning all of the nonlinear dynamic features of the PAM robot arm because the predictive capability of the recurrent first order NARX structure and of the recurrent second order NARX structure permit both to thorough learn all of the highly nonlinear and dynamic features of the PAM robot arm.

Finally, the convergence of the principal parameters of the proposed PAM robot arm inverse NARX11 and inverse NARX22 fuzzy models (including the convergence of the number of input and output membership functions; the convergence of the theta-parameter of the rule-base; the convergence of the scaling gain of the input-output variables; the convergence of the spacing-parameter determining the shape of the input-output membership functions; and the convergence of the spacing-parameter determining the structure of the rule-base of the input-antecedents and output-consequent) identified and optimized by the MGA are shown in Figs.13d and Fig.15e, respectively. From the theta-angle parameter and the spacing parameter of the input-output rule base identified by the MGA, the derived resulting rule-base of the desired inverse NARX11 fuzzy model is shown in Table 3. It is composed of 25 rules from two input variables (*Y(z)*[deg] and *U(z-1)*[V]) that both possessed MF numbers of 5.

Next Subsection 5.2 will experimentally prove the good performance of the novel INFM not only in modeling and identification but also in control. The novel INFM will be applied in the proposed hybrid inverse NARX fuzzy-PID control scheme.

5.2. Experimental Results of the PAM Robot Arm Hybrid Inverse NARX Fuzzy-PID Position Control:

The second joint of the PAM robot arm is considered as a case study to apply this control technique. The performance of the novel proposed hybrid inverse NARX fuzzy-PID control scheme is verified on the position joint angle control of the second joint of the PAM robot arm. Fig.8 describes the working diagram of this control scheme.

The proposed hybrid inverse NARX11 fuzzy-PID control algorithm runs in real-time windows target (RWT) platform of the MATLAB-SIMULINK environment with the inverse NARX11 fuzzy model being an MGA-based optimized fuzzy inference system (FIS) structure as described in Figs 14 and 15. The PID controller is implemented in parallel with the inverse NARX fuzzy to compensate and keep the PAM system stable during starting time. Three PID parameters are chosen by trial and error method and are determined as K_P=0.09; K_I=0.089 and K_D=0.02.

The final purpose of the PAM robot arm is to be used as an elbow and wrist rehabilitation robot device. Thus, the experiments were carried out with respect to three different waveforms as reference inputs (triangular, trapezoidal and sinusoidal reference) with two different end-point payloads (load 0.5[kg] and load 2[kg]) to demonstrate the performance of the novel proposed hybrid inverse NARX fuzzy-PID controller. Furthermore, comparisons of the control performance were performed between the conventional PID and the two different methods of the proposed hybrid inverse NARX fuzzy-PID controller.

These two novel proposed methods were composed of the proposed hybrid inverse NARX11 fuzzy-PID and proposed hybrid inverse NARX22 fuzzy-PID. The first method possesses the nonlinear first order NARX model in the MGA-based inverse NARX11 fuzzy model and the second method corresponds to the nonlinear second order NARX model implied in the MGA-based inverse NARX22 fuzzy model.

The initial value K and the PID controller parameters K_p, K_i and K_d were set to be K = 0.6, Kp = 0.089, Ki = 0.09, and Kd = 0.02. These PID controller parameters were obtained by trial and error through experiment.

First, the experiments were carried out to verify the effectiveness of the proposed hybrid inverse NARX fuzzy-PID controller with the triangular reference input. Fig.16a compares the experimental

results between the conventional PID controller and the proposed hybrid inverse NARX fuzzy-PID controller in the two cases of load 0.5[kg] and load 2[kg], respectively.

This figure shows that due to the good dynamic approximation of the INFM which adapts well to the payload variation and nonlinear disturbances of the PAM system in its operation, the error between the desired reference y_{REF} and the actual joint angle response y of the PAM manipulator were optimized. Consequently, the minimized error is obtained only in the range ± 0.8[deg] for both the proposed hybrid inverse NARX11 fuzzy-PID and the hybrid inverse NARX22 fuzzy-PID in the case of load 0.5[kg]. The same good result is obtained with both of the proposed control scheme in the case of load 2[kg]. These results are very impressive in comparison with the bad error of the conventional PID controller (± 2.5[deg] in both of case).

The comparison between the proposed hybrid inverse NARX11 fuzzy-PID and hybrid inverse NARX22 fuzzy-PID showed that both of the proposed control algorithms obtain the good robustness and accuracy as well and thus are considered to obtain the performance equivalent.

Figure 16b shows the resulted shape of the control voltage U applied to the joint of the PAM robot arm, which is generated by the proposed Hybrid Inverse NARX Fuzzy-PID controller to assure the performance and accuracy of the PAM robot arm response. This control voltage U is composed of U_{PID} and U_{FUZZY}. The control voltage U_{PID} is used to compensate the variation of the reference signal and of the two different payloads while U_{FUZZY} is used to ameliorate the response accuracy and to keep the PAM system operation stable.

Next, the experiments were carried out to verify the effectiveness of the proposed Hybrid Inverse NARX Fuzzy-PID controller with the trapezoidal reference input. Fig.17a shows the experimental results comparison between the conventional PID controller and the two proposed hybrid inverse NARX11 fuzzy-PID and hybrid inverse NARX22 fuzzy-PID controllers in the two cases of load 0.5[kg] and load 2[kg] respectively.

These results show that due to the good dynamic approximation of the INFM which adapts well to the different payloads and nonlinear disturbances of the PAM system in its operation, the error between the desired reference y_{REF} and the actual joint angle response y of the PAM robot arm were optimized. Consequently, the minimized error is obtained only in the range ± 0.7[deg] with both of the proposed control scheme in the case of load 0.5[kg] and only in the range ± 0.6[deg] with both of proposed control scheme in case of load 2[kg]. These results are very superior in comparison with the disappointing error of the conventional PID controller (± 2[deg] for the case of load 0.5[kg] and up to ± 2.2[deg] for the case of load 2[kg]).

Figure 17b shows the resulted shape of the control voltage U applied to the joint of the PAM manipulator, which is generated by the proposed Hybrid Inverse NARX Fuzzy-PID controller to assure the performance and accuracy of the PAM manipulator response. This control voltage U is composed of U_{PID} and U_{FUZZY}. The control voltage U_{PID} is used to compensate the variation of the reference signal and the different payloads while U_{FUZZY} is used to ameliorate the response accuracy and to keep the PAM system operation stable. Likewise, the proposed hybrid inverse NARX fuzzy-PID controller assures to robustly control with the refined control voltage as to keep the PAM robot arm response stable and accurate tracking.

Finally, the experiments were carried out to verify the effectiveness of the proposed Hybrid Inverse NARX Fuzzy-PID controller with the sinusoidal reference 0.05[Hz]. Fig.18 compares the experimental results between the conventional PID controller and the two proposed control scheme in the two cases of load 0.5[kg] and load 2[kg], respectively.

These results show that due to the good approximation and robustness of the INFM, which adapts well to the different payloads and the disturbance variation of the PAM system in its operation, the error between the desired reference y_{REF} and the actual joint angle response y of the PAM robot arm is optimized. As a result, the error is well minimized in the range ± 2[deg] in the case of load 0.5[kg], in the range ± 1.8[deg] with the proposed hybrid inverse NARX11 fuzzy-PID and ± 1.4[deg] with the proposed hybrid inverse NARX22 fuzzy-PID in the case of load 2[kg]. These results are very superior in comparison with the passive error of the conventional PID controller (± 4[deg] in the case of load 0.5[kg] and up to ± 3.4[deg] in the case of load 2[kg]).

The comparison between the proposed hybrid inverse NARX11 fuzzy-PID and hybrid inverse NARX22 fuzzy-PID shows that the proposed hybrid inverse NARX22 fuzzy-PID obtains both of excellent robustness and good accuracy slightly better in comparison with the proposed hybrid inverse NARX11 fuzzy-PID and thus the proposed hybrid inverse NARX22 fuzzy-PID controller is considered to possess the best performance. However, the proposed hybrid inverse NARX11 fuzzy-PID controller proves to have the advantage due to its simple fuzzy FIS structure.

In summary, Table 4 tabulates all of the principal results of the MGA-based PAM robot arm INFM identification. Based on the fitness convergence as well as the related important parameters shown in Figs.12 and 13 for the novel proposed MGA-based Inverse NARX11 Fuzzy model identification, and Figs.14 and 15 with good results in the case of the novel proposed MGA-based inverse NARX22 fuzzy model identification, it can be concluded that the MGA-based inverse fuzzy model identification algorithm, which very poorly obtains the training performance is quite inferior in comparison with the novel proposed MGA-based INFM identification algorithm not only in the speed of convergence but

also in performance. Furthermore, it is also shown that the proposed method had a good control performance for the highly nonlinear system, such as the PAM robot arm. The controller had an adaptive control capability when the control parameters were offline optimized via the modified genetic algorithm (MGA). The controller designed by this method only needs a training procedure in advance, but it uses only the input and output training data from the plant for the adaptation of the proposed INFM. From the experiments of the position control of the PAM robot arm, it was verified that the proposed control algorithm presented in this paper was precisely and robustly controlled with a simple structure and obtained a better dynamic property, good robustness and it was suitable for the control of various plants, including the linear and nonlinear processes, compared to the conventional PID controller.

6. CONCLUSIONS

Whereas expert knowledge is usually required to design a fuzzy model using traditional methods, this paper shows that it is capable even without using any knowledge of the system except the experiment input-output training data. The novel proposed MGA can build an effective INFM model obtaining superb features both in convergence speed and in improving performance. This novel proposed technique may leads to an increase in the use of the proposed NARX fuzzy model, as the previously time-consuming design procedure can be reduced spectacularly, not only in modeling, simulation and identification of the highly nonlinear systems, but also in the online adaptive and predictive control of the dynamic nonlinear systems in general and the PAM robot arm in particular. Furthermore the performance of the proposed Hybrid Inverse NARX Fuzzy-PID controller was found to be very good and robust in the presence of intrinsic and external disturbances. This facilitates testing under different input conditions and ensures future applications of the PAM robot arm as a rehabilitation device for stroke patients. It determines confidently that the proposed Hybrid Inverse NARX Fuzzy-PID controller not only proves its good performance in control of the highly nonlinear PAM robot arm but also is very efficient in the control of other real-time industrial and human-friendly applications.

ACKNOWLEDGEMENTS

This research was supported by the NAFOSTED, Viet Nam and the Brain Korea 21 (BK21), Republic of Korea.

REFERENCES

Ahn K.K., Anh H.P.H., 2006. System modeling and identification of the two-link pneumatic artificial muscle (PAM) manipulator optimized with genetic algorithm. In: Proceedings of the 2006 IEEE-ICASE Int. Conf., Busan, Korea, pp. 356–61.

Ahn K.K., Anh H.P.H., 2007a. Modeling and adaptive self-tuning MVC of the 2-axes pneumatic artificial muscle (PAM) manipulator optimized with genetic algorithm." In KSME Journal 2007 (Submitted).

Ahn K.K., Anh H.P.H., 2007b. A new approach of modeling and identification of the pneumatic artificial muscle (PAM) manipulator based on recurrent neural network. In Proc. IMechE, Part I: Journal of Systems and Control Engineering, 2007, 221(I8), 1101-1122.

Ahn K.K., Anh H.P.H., 2009. Identification of the pneumatic artificial muscle manipulators by MGA-based nonlinear NARX fuzzy model. In MECHATRONICS, 2009, Volume 19, Issue 1, pp. 106-133.

Ahn K.K., Thanh T.D.C., 2005. Nonlinear PID control to improve the control performance of PAM manipulators using neural network. In KSME, Int., Jour., 19(1):pp.106~15.

Ahn K.K., Thanh T.D.C., 2006. Intelligent phase plane switching control of pneumatic artificial muscle manipulators with magneto-rheological brake. In Mechatronics, March 16(2):pp.85-95.

Back T., Hoffmeister F., 2001. Extended Selection Mechanism in Genetic Algorithm. In: Proceedings of the 4th IEEE Int. Conf. of Genetic Algorithms, Univ. of California, CA, U.S.A., pp. 89-99.

Balasubramanian K, Rattan K.S., 2003a. Fuzzy logic control of a pneumatic muscle system using a linearizing control scheme. In: Proceedings of Int. Conf., North American Fuzzy Information Processing Society, pp. 432-6.

Balasubramanian K, Rattan K.S., 2003b. Feed-forward control of a non-linear pneumatic muscle system using fuzzy logic. In: Proceedings of IEEE Int., Conf., Fuzzy Systems. 1:pp.272-7.

Boerlage, M., Steinbuch, M., Lambrechts, P. and van de Wal, M., 2003, Model – Based Feedforward for Motion Systems. Proceedings of IEEE Conference on Control Applications, **1**, pp. 1158–1163.

Caldwell D.G., Medrano-Cerda G.A., Goodwin M., 1995. Control of pneumatic muscle actuators. IEEE Trans. Control Syst. Mag., Feb. 15(1):pp.40–8.

Chan S.W., Lilly J., Berlin J.E., May 2003. Fuzzy PD+I learning control for a pneumatic muscle. In: Proceedings of IEEE Int. Conf. Fuzzy Systems, St. Louis, MO, pp. 278–83.

Chen T.Y., Chen C.J., Feb 2000. Improvement of simple genetic algorithm in structural design. Int. J. for Numerical Methods in Engineering, 40:pp.1323-34.

Cheong F., Lai R., Feb 2000. Constraining the Optimization of a Fuzzy Logic Controller Using an Enhanced Genetic Algorithm. IEEE Transactions on Systems, Man and Cybernetics-Part B: Cybernetics, pp. 30(1).

Chou C.P., Hannaford B., 1994a. A study of pneumatic muscle technology for possible assistance in mobility. In: Proceedings of 19th Annu. Int. Conf. the IEEE Engineering in Medicine and Biology Soc., Chicago, IL, pp. 1884–7.

Chou C.P., Hannaford B., 1994b. Static and dynamic characteristics of McKibben pneumatic artificial muscles. In: Proceedings of the 1994 IEEE Robotics and Automation Conf., pp. 281–6.

Cocatre-Zilgien J.H., Delcomyn F, Hart J.M., 1996. Performance of a muscle-like 'leaky' pneumatic actuator powered by modulated air pulses. IEEE J. Robot. Syst., 13(6):pp.379–90.

Hesselroth T, Sarkar K, Van der Smagt P, Schulten K., 1994. Neural network control of a pneumatic robot arm. IEEE Trans. System Man Cybernetics 24(1): pp.28–38.

Lilly J., Sep. 2003.Adaptive tracking for pneumatic muscle actuators in bicep and tricep configurations. IEEE Trans. Neural Syst. Rehabil. Eng. 11(3):pp.333–9.

Lilly J.H., Chang X., Sep.2003. Tracking control of a pneumatic muscle by an evolutionary fuzzy controller. In IEEE Intell. Automat. Soft Comput., 9(3):pp. 227–44.

Medrano-Cerda G.A., Bowler C.J., Caldwell D.G., Aug. 1995. Adaptive position control of antagonistic pneumatic muscle actuators. In: Proceedings of IEEE Int. Conf. Intelligent Robots and Systems, Pittsburgh, PA, pp. 378–83.

Nelles O., Nonlinear system identification, Springer, 2000.

Pack R.T., Christopher J.J.L., Kawamura K., Apr. 1997. A rubbertuator-based structure climbing inspection robot. In: Proceedings of IEEE Int. Conf. Robotics and Automation, vol. 3, Albuquerque, NM, pp. 1869–74.

Park Y.J., Cho H., Cha D.H., 1995. Genetic algorithm-based optimization of fuzzy logic controller using characteristic parameters. In: Proceedings of the IEEE International Conference on evolutionary Computation, pp. 831-6

Potts J.C., Giddens T.D., Yadav S.B., 1994. The Development and Evaluation of an Improved GA Based on Migration and Artificial Selection. IEEE Trans. Systems Man Cybernetics, 24(1):pp.73-86.

Repperger D.W., Johnson K.R., Phillips C.A., 1998. VSC position tracking system involving a large scale pneumatic muscle actuator. In: Proceedings of IEEE Conf. Decision Control, Tampa, FL, Dec. pp. 4302–7.

Repperger D.W., Phillips C.A., Krier M., Aug. 1999. Controller design involving gain scheduling for a large scale pneumatic muscle actuator," In: Proceedings of IEEE Conf. Control Applications, Kohala Coast, HI, pp. 285–90.

Reynolds D.B., Repperger D.W., Phillips C.A., Bandry G., 2003. Dynamic characteristics of pneumatic muscle. In IEEE Ann. Biomed. Eng., 31(3):pp.310–7.
Tsagarakis N, Darwin G.C., 2000.Improved modeling and assessment of pneumatic muscle actuators. In: Proceedings of IEEE Int. Conf. Robotics and Automation, San Francisco, CA, pp. 3641–6.

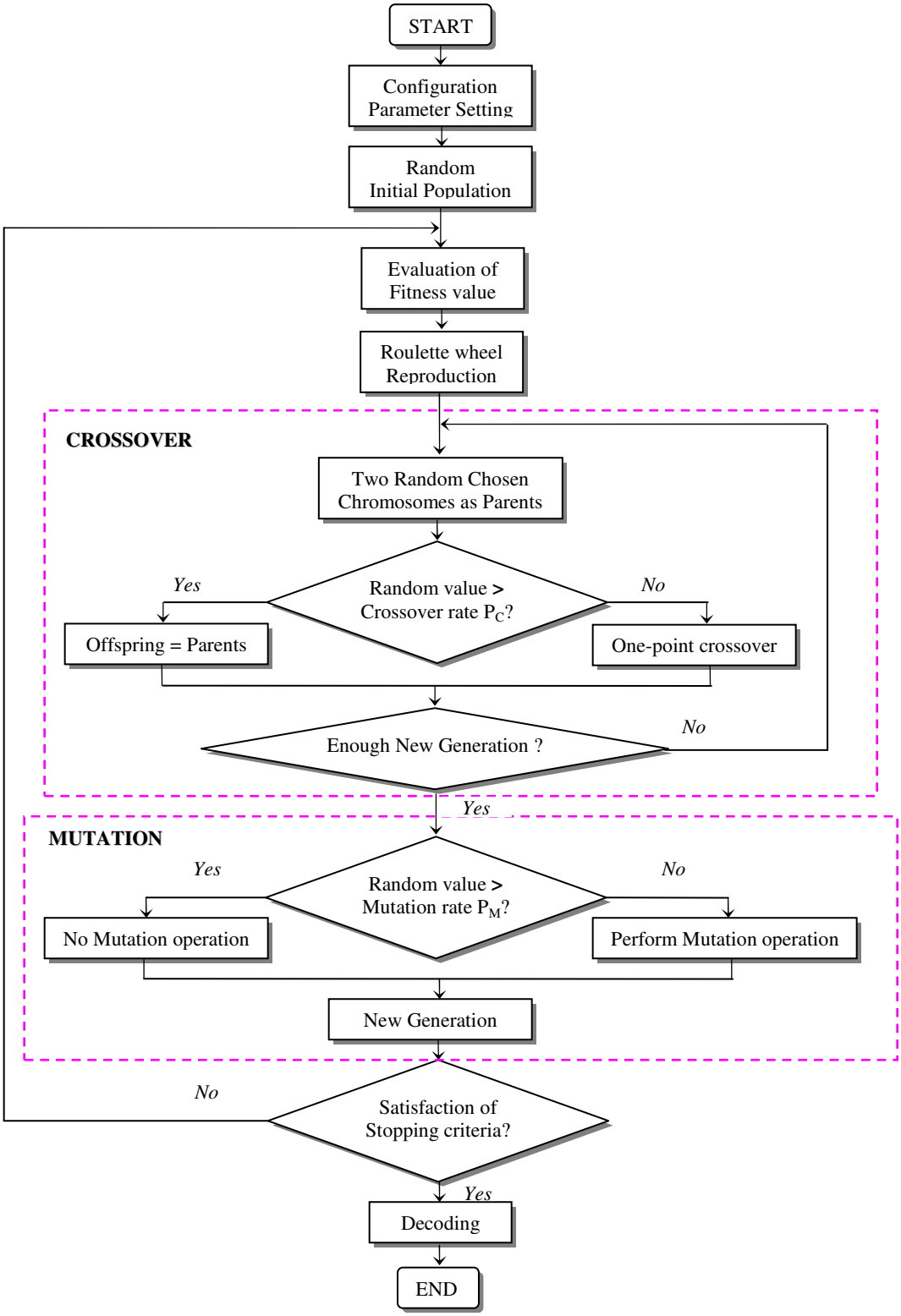

Figure 1: The flow chart of the conventional GA optimization procedure.

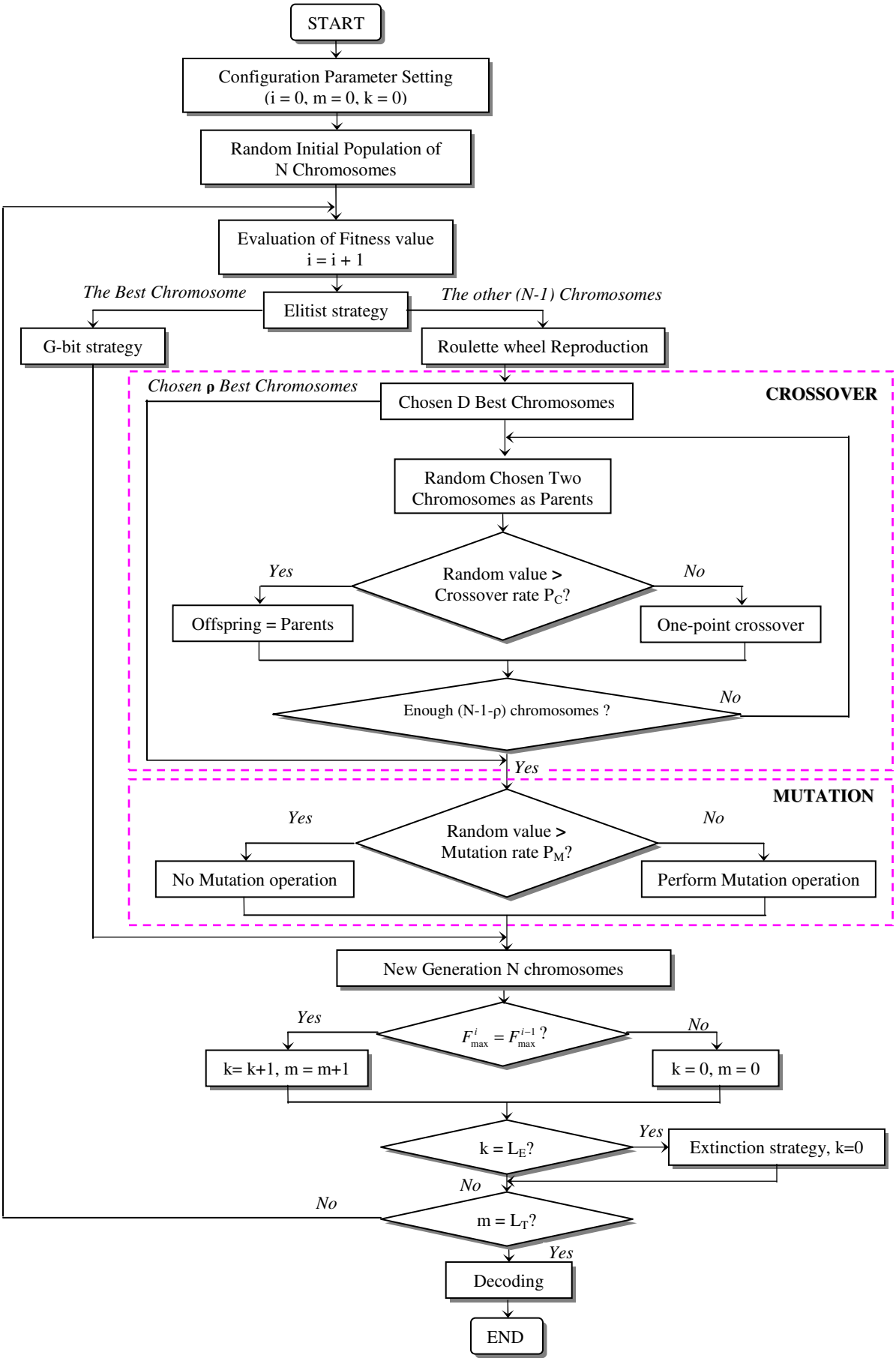
START
Configuration Parameter Setting
(i = 0, m = 0, k = 0)
Random Initial Population of
N Chromosomes
Evaluation of Fitness value
i = i + 1
The Best Chromosome
Elitist strategy
The other (N-1) Chromosomes
G-bit strategy
Roulette wheel Reproduction
Chosen ρ Best Chromosomes
Chosen D Best Chromosomes
CROSSOVER
Random Chosen Two
Chromosomes as Parents
Yes
Random value >
Crossover rate P_C?
No
Offspring = Parents
One-point crossover
Enough (N-1-ρ) chromosomes ?
No
Yes
MUTATION
Yes
Random value >
Mutation rate P_M?
No
No Mutation operation
Perform Mutation operation
New Generation N chromosomes
Yes
$F^i_{max} = F^{i-1}_{max}$?
No
k= k+1, m = m+1
k = 0, m = 0
k = L_E?
Yes
Extinction strategy, k=0
No
No
m = L_T?
Yes
Decoding
END

Figure 2: The flow chart of the modified genetic algorithm (MGA) optimization procedure.

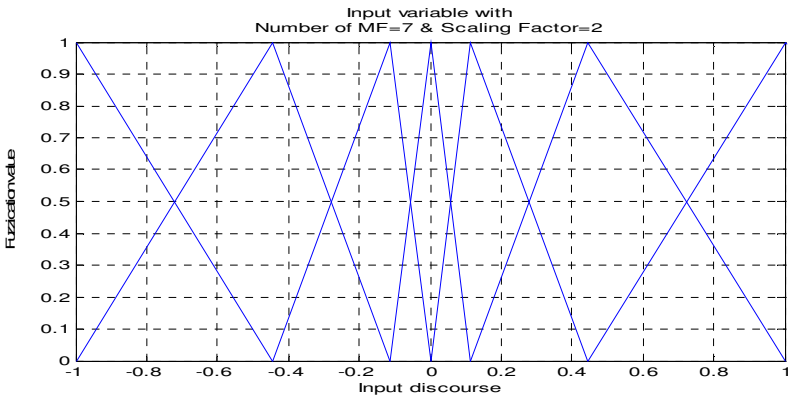

Figure 3: Triangle input membership function with spacing factor = 2.

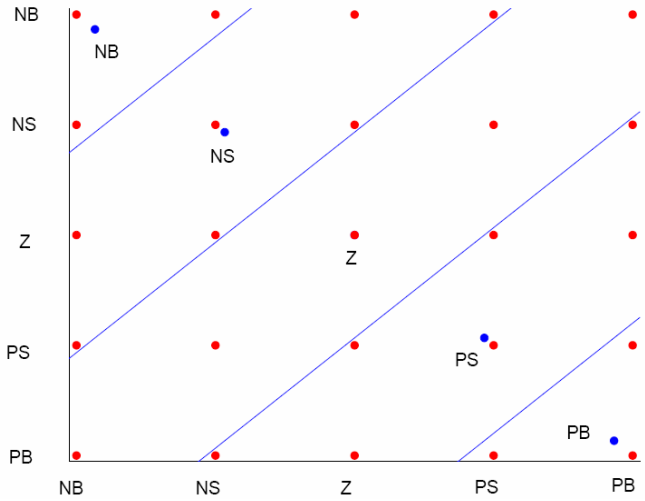

Figure 4a: The seed points and the grid points for rule-base construction

de \ e	NB	NS	Z	PS	PB
NB	NB	NB	NS	NS	Z
NS	NB	NS	NS	Z	PS
Z	NS	NS	Z	PS	PS
PS	NS	Z	PS	PS	PB
PB	Z	PS	PS	PB	PB

Figure 4b: Derived rule base

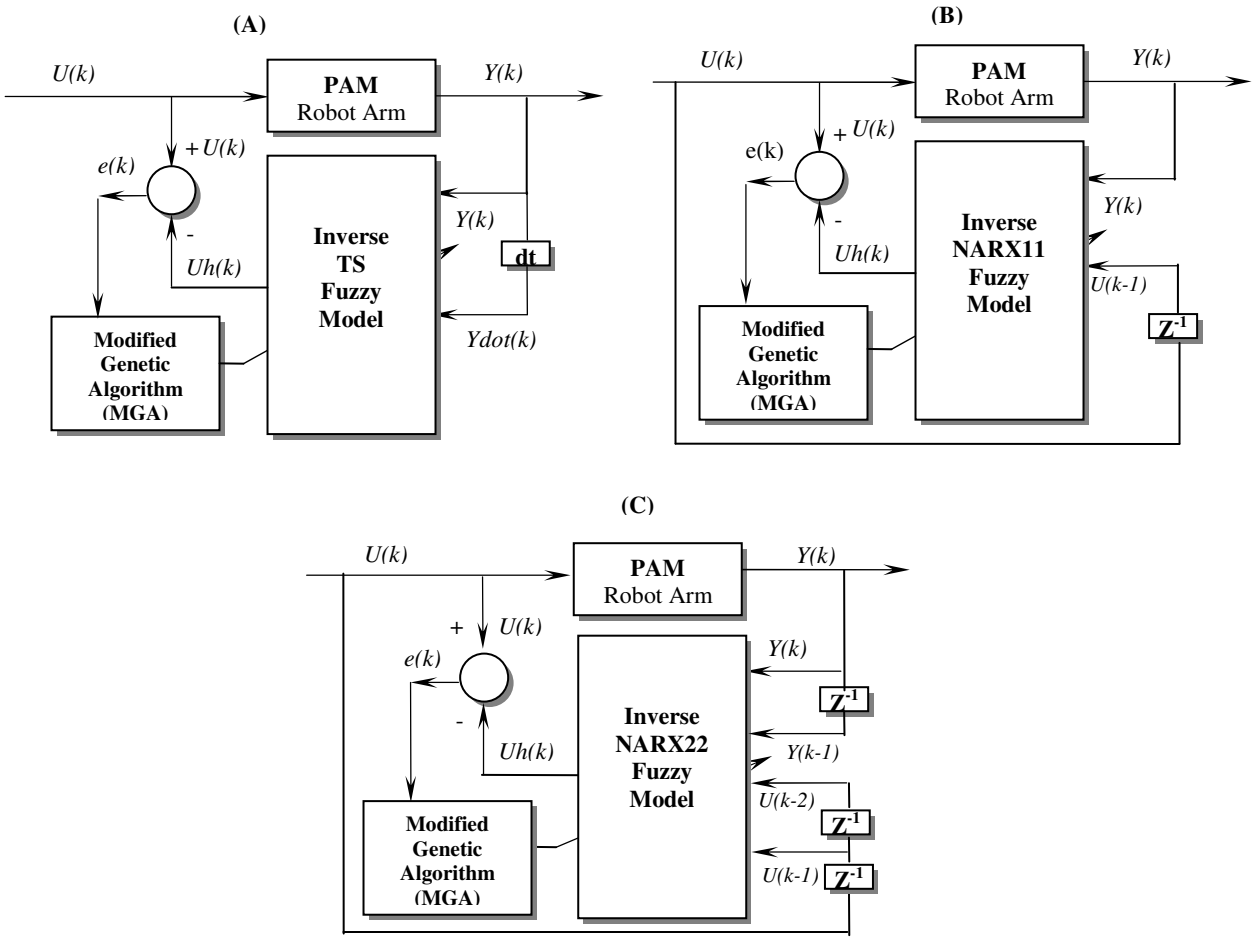

Figure 5: Block diagrams of the MGA-based PAM robot arm Inverse Fuzzy Model Identification

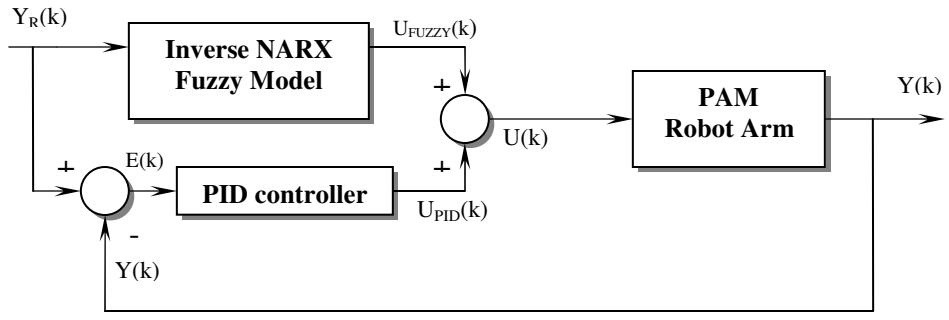

Figure 6.Block diagram of the proposed PAM robot arm Hybrid Inverse NARX Fuzzy -PID control system

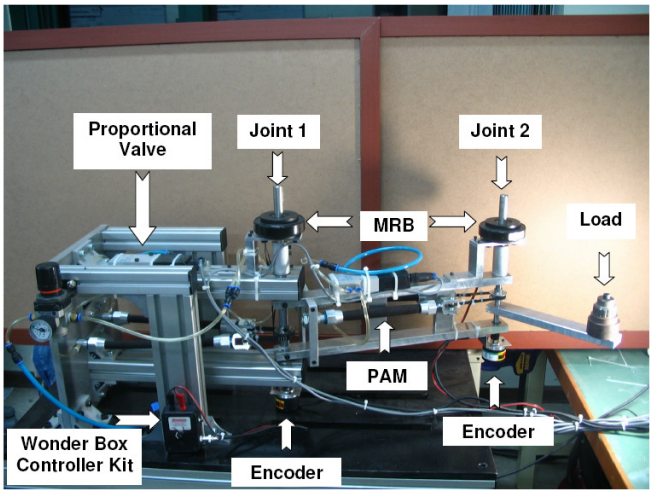

Figure 7: Photograph of the experimental two-axes PAM robot arm

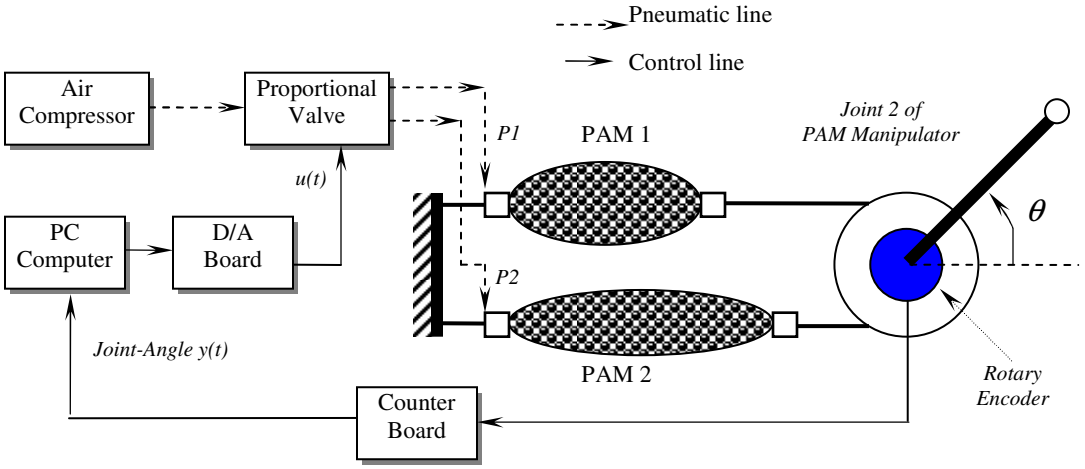

Figure 8: Block diagram for the working principle of the second joint of the 2-axes PAM robot arm.

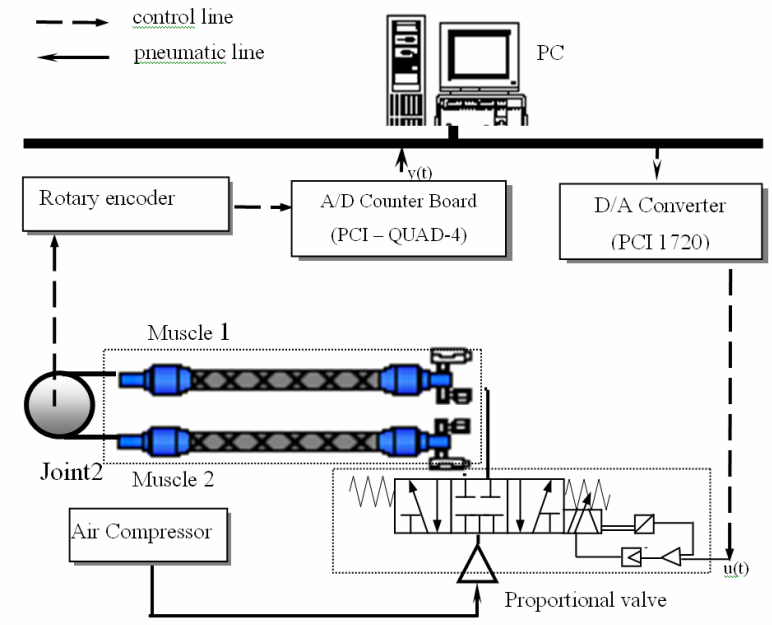

Figure 9. Schematic diagram of the experimental apparatus

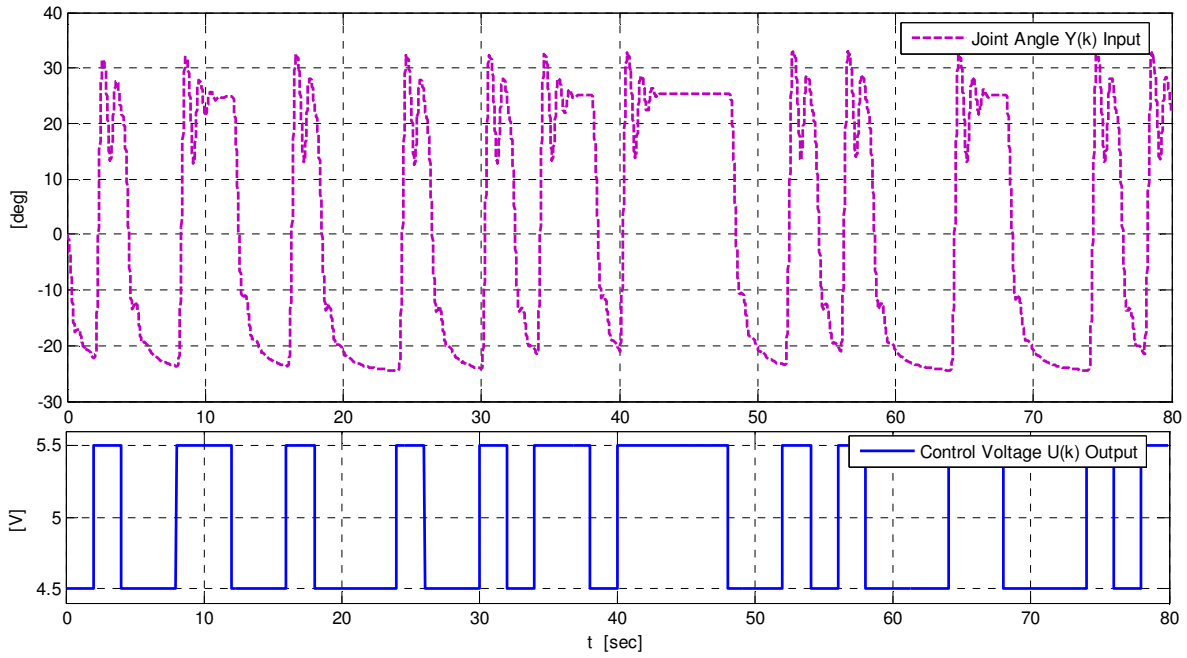

Figure 11: Inverse NARX Fuzzy Model Training data obtained by experiment.

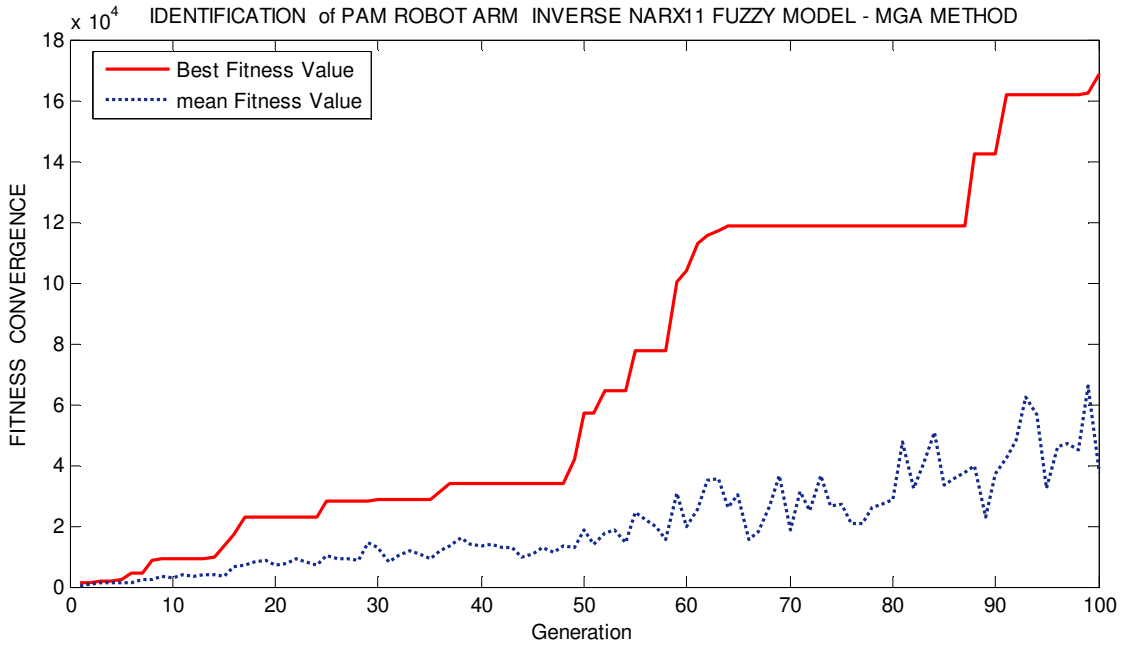

Figure 12. Fitness Convergence MGA-based Inverse NARX11 Fuzzy Model Identification of the PAM robot arm (Using MGA Method with Population=20; Generation=100; Fitness=168800).

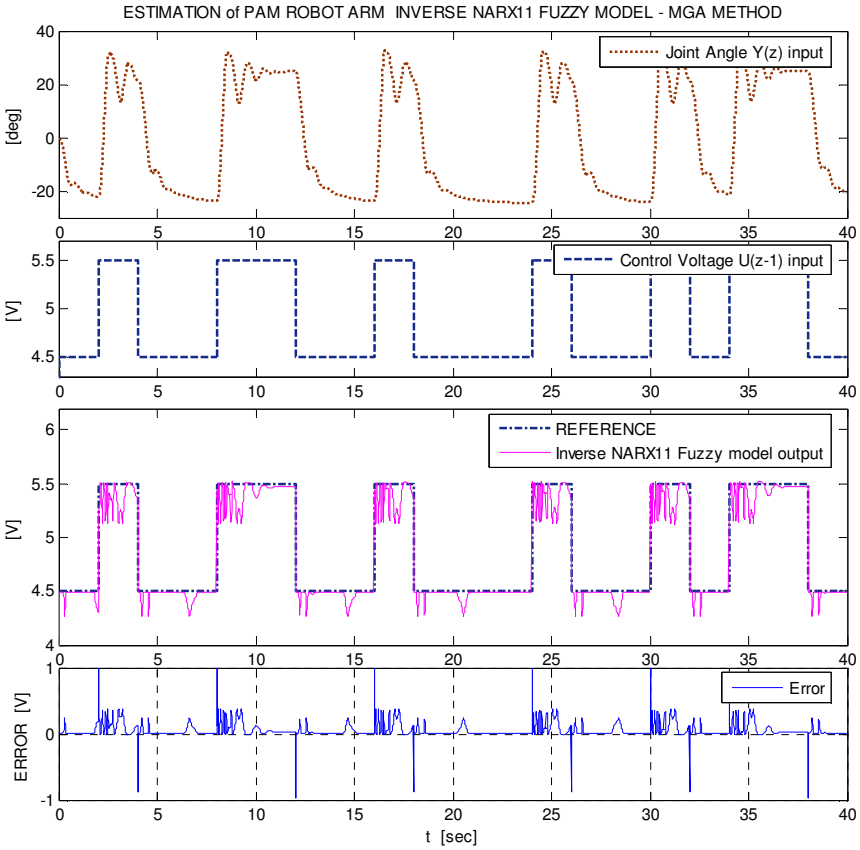

Figure 13a. Estimation of MGA-based Inverse NARX11 Fuzzy Model of the PAM robot arm

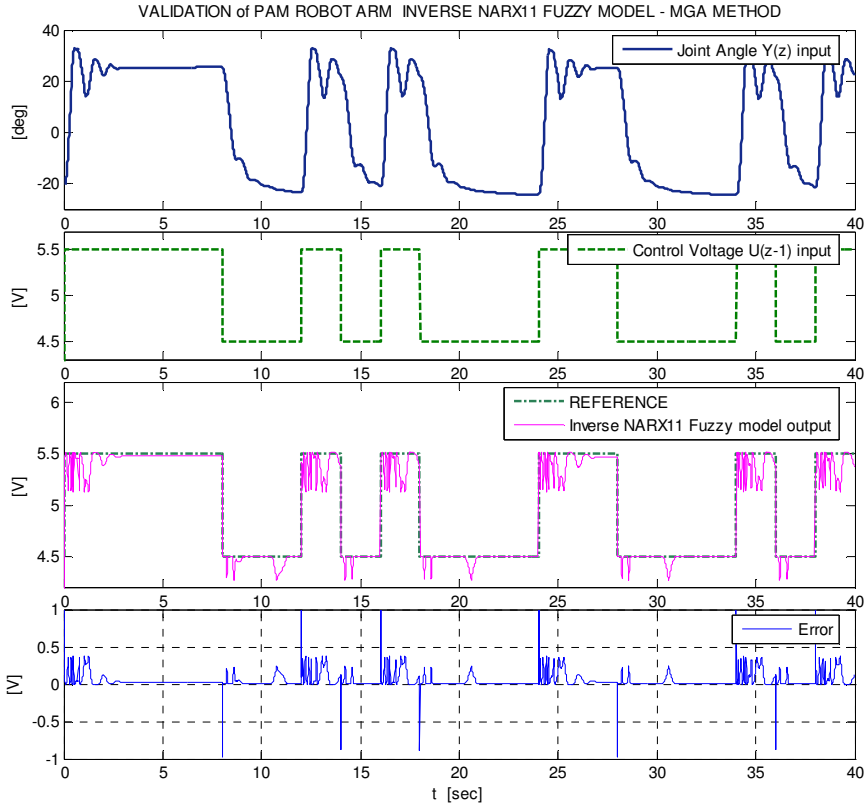

Figure 13b. Validation of MGA-based Inverse NARX11 Fuzzy Model of the PAM robot arm

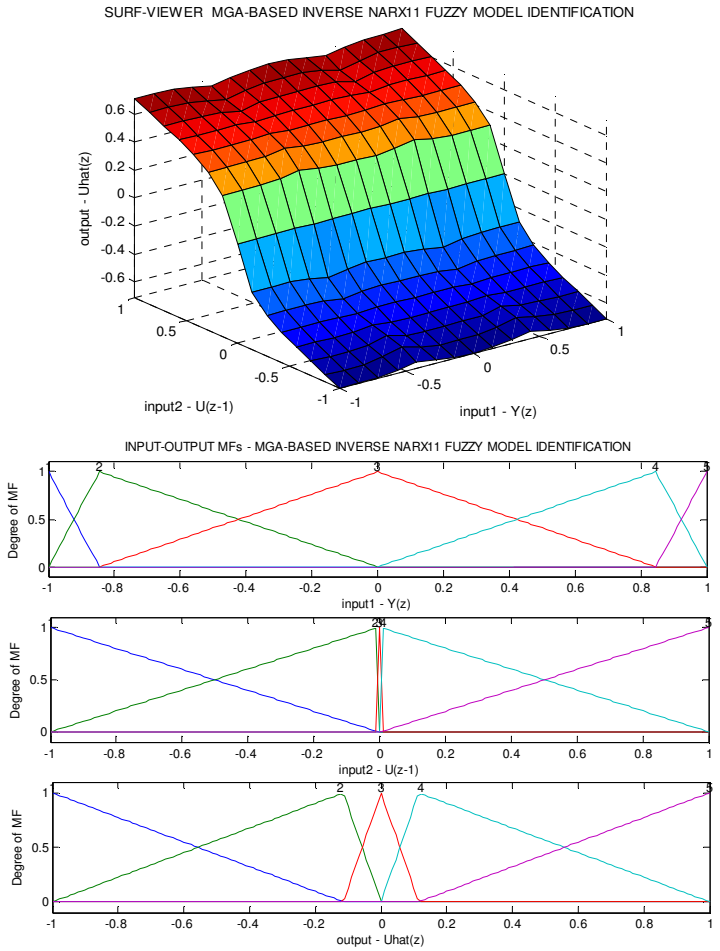

Figure 13c. Membership Input-Output & Surf-View of MGA-based Inverse NARX11 Fuzzy Model Identification

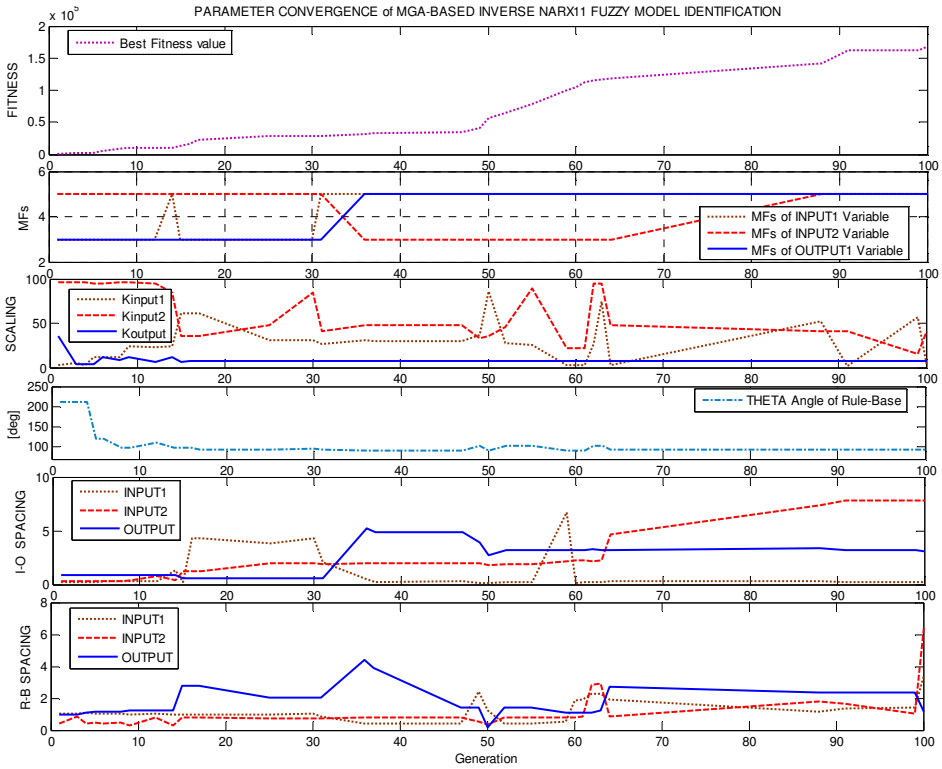

Figure 13d. Convergence of Principal Parameters of MGA-based Inverse NARX11 Fuzzy Model Identification

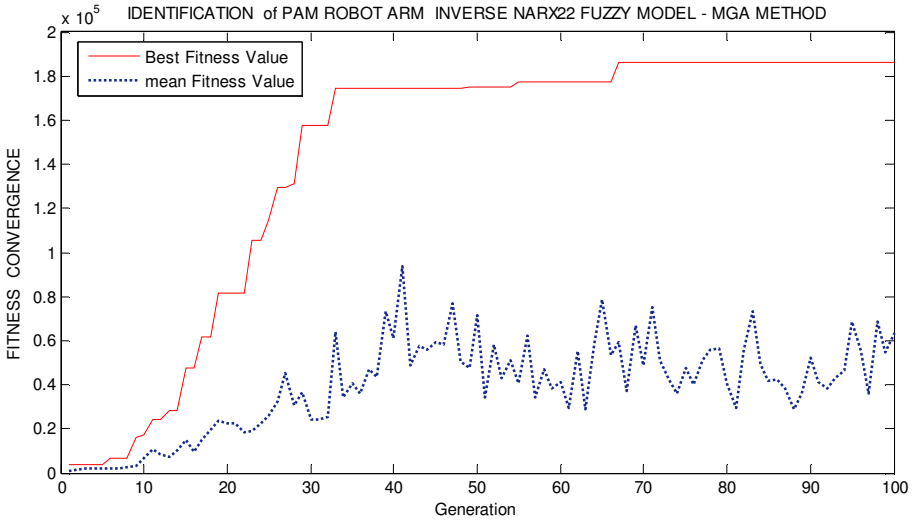

Figure 14. Fitness Convergence MGA-based Inverse NARX22 Fuzzy Model Identification of the PAM robot arm (Using MGA Method with Population=20; Generation=100; Fitness=186042).

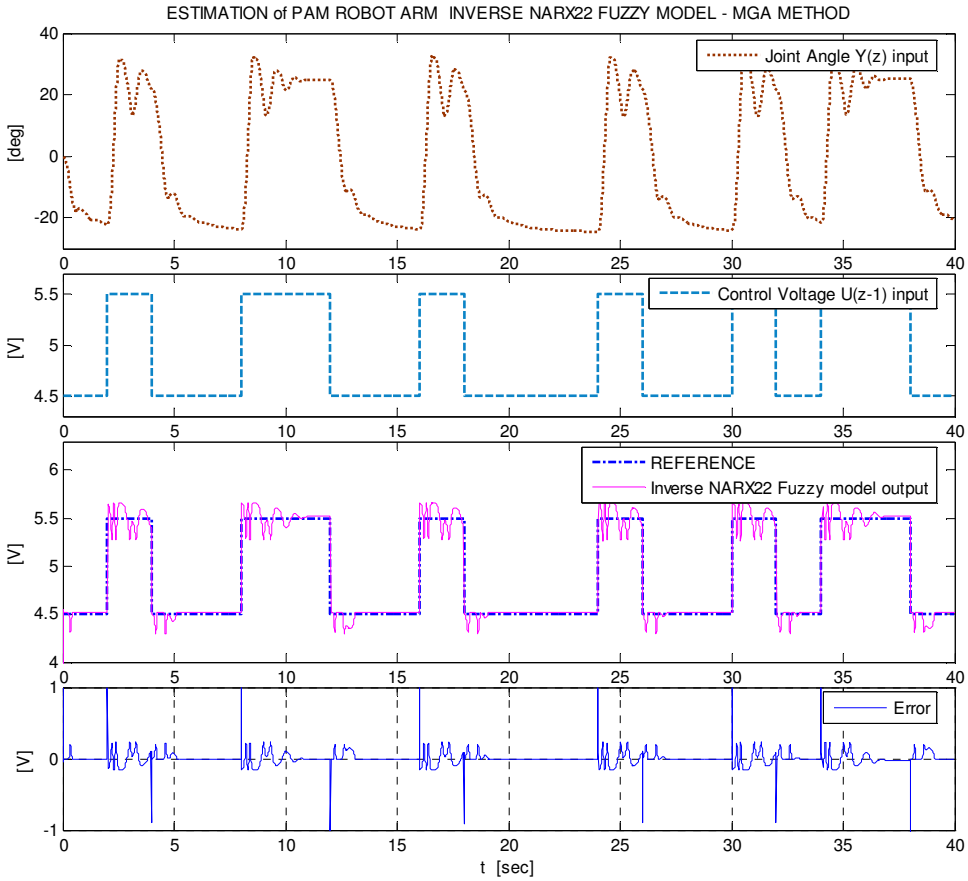

Figure 15a. Estimation of MGA-based Inverse NARX22 Fuzzy Model of the PAM robot arm

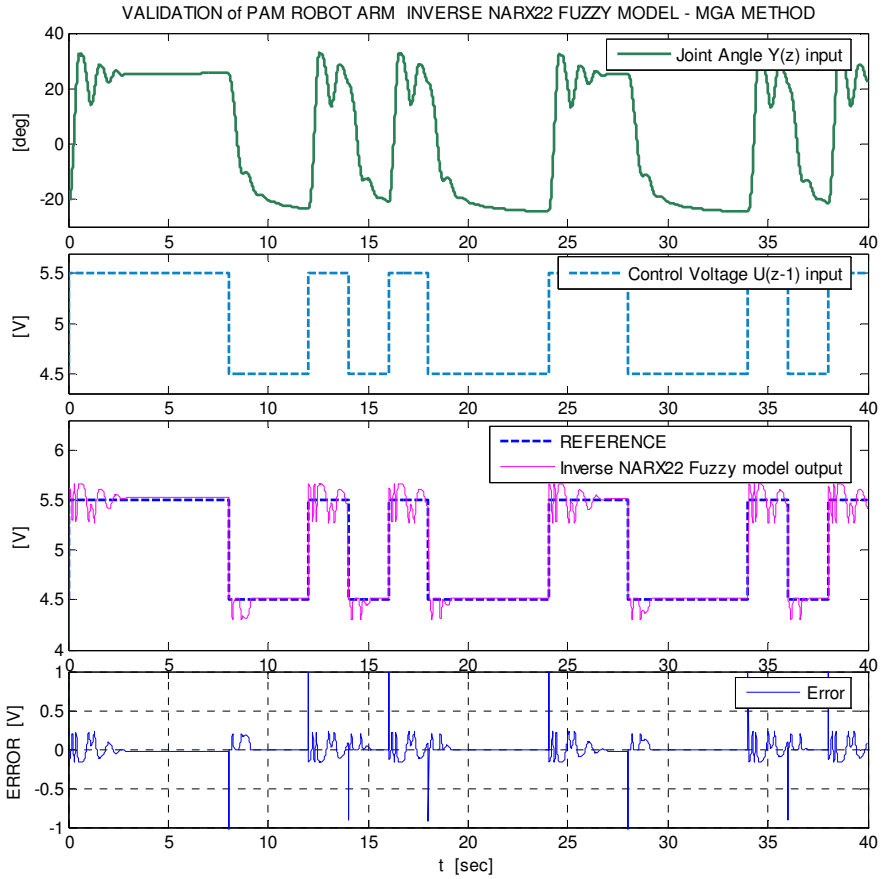

Figure 15b. Validation of MGA-based Inverse NARX22 Fuzzy Model of the PAM robot arm

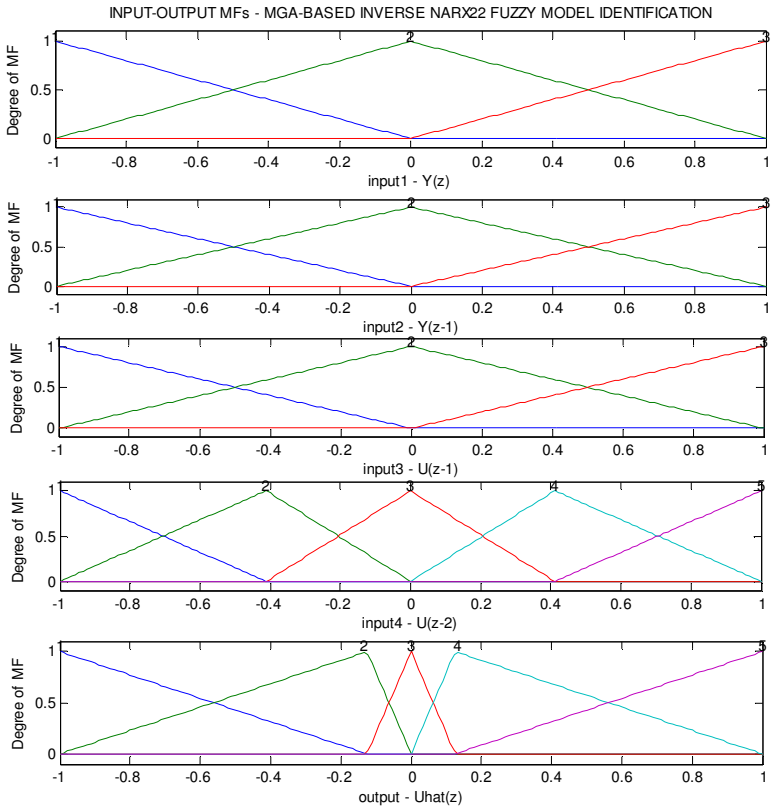

Figure 15c. Membership Input-Output of MGA-based Inverse NARX22 Fuzzy Model Identification

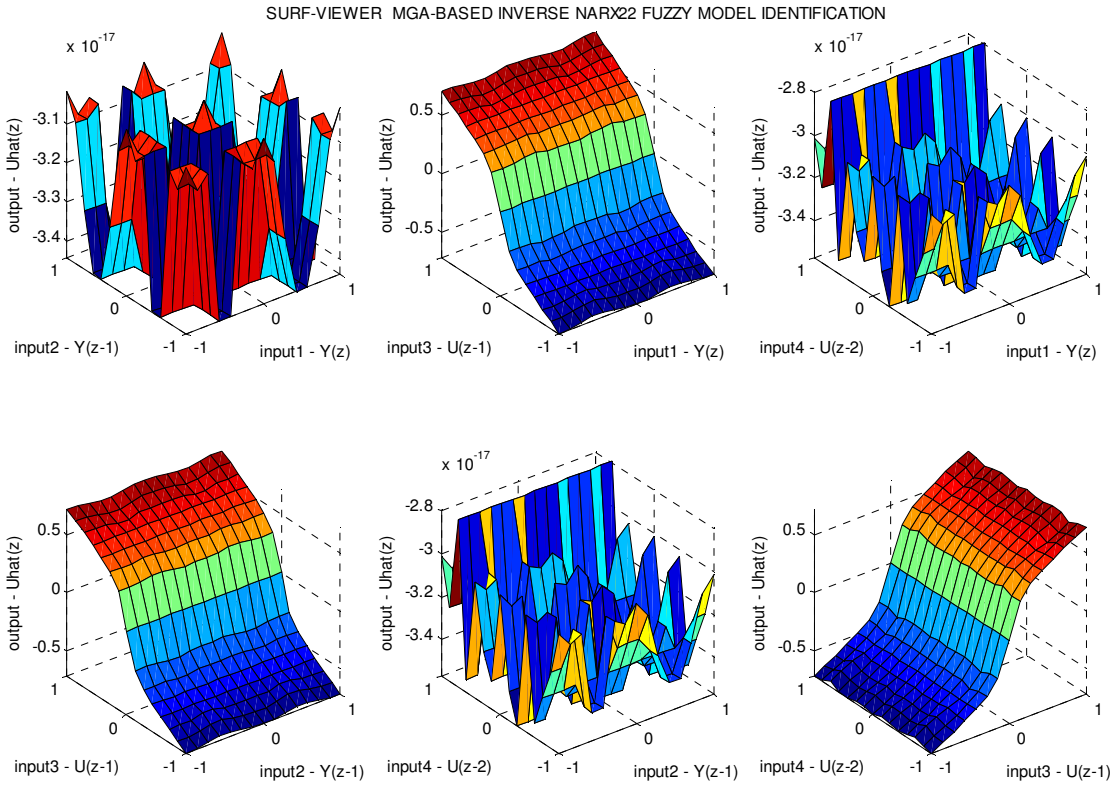

Figure 15d. Rule Base Surf-Viewer of MGA-based Inverse NARX22 Fuzzy Model Identification

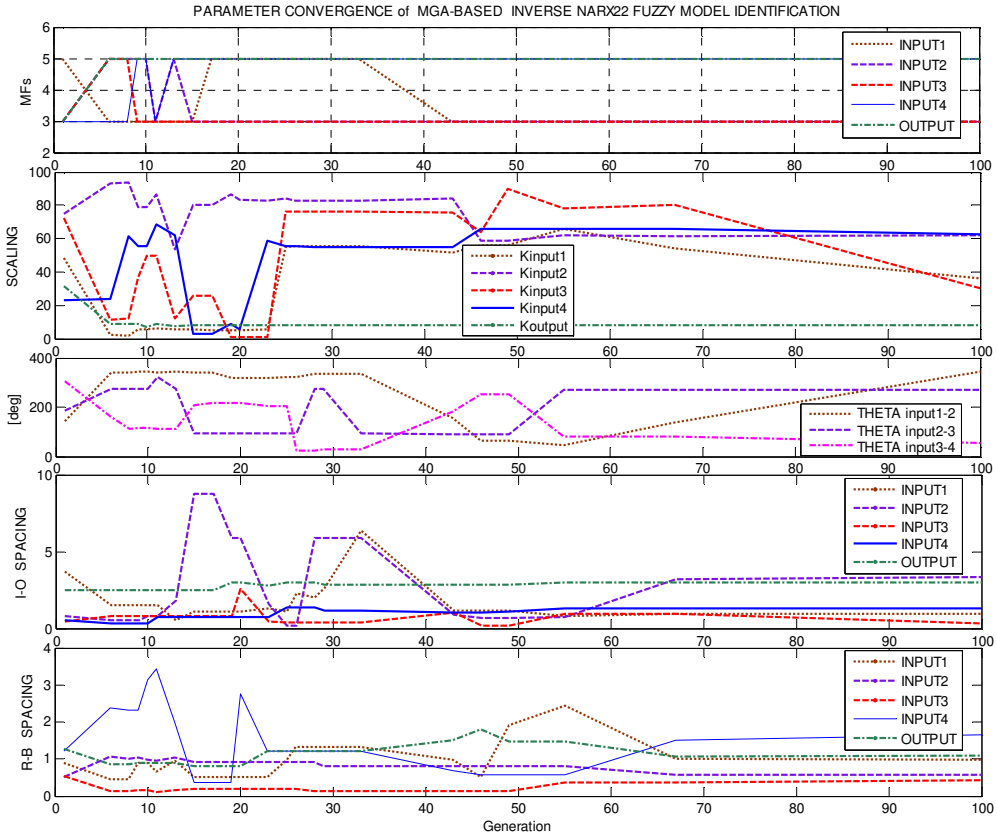

Figure 15e. Convergence of Principal Parameters of MGA-based Inverse NARX22 Fuzzy Model Identification

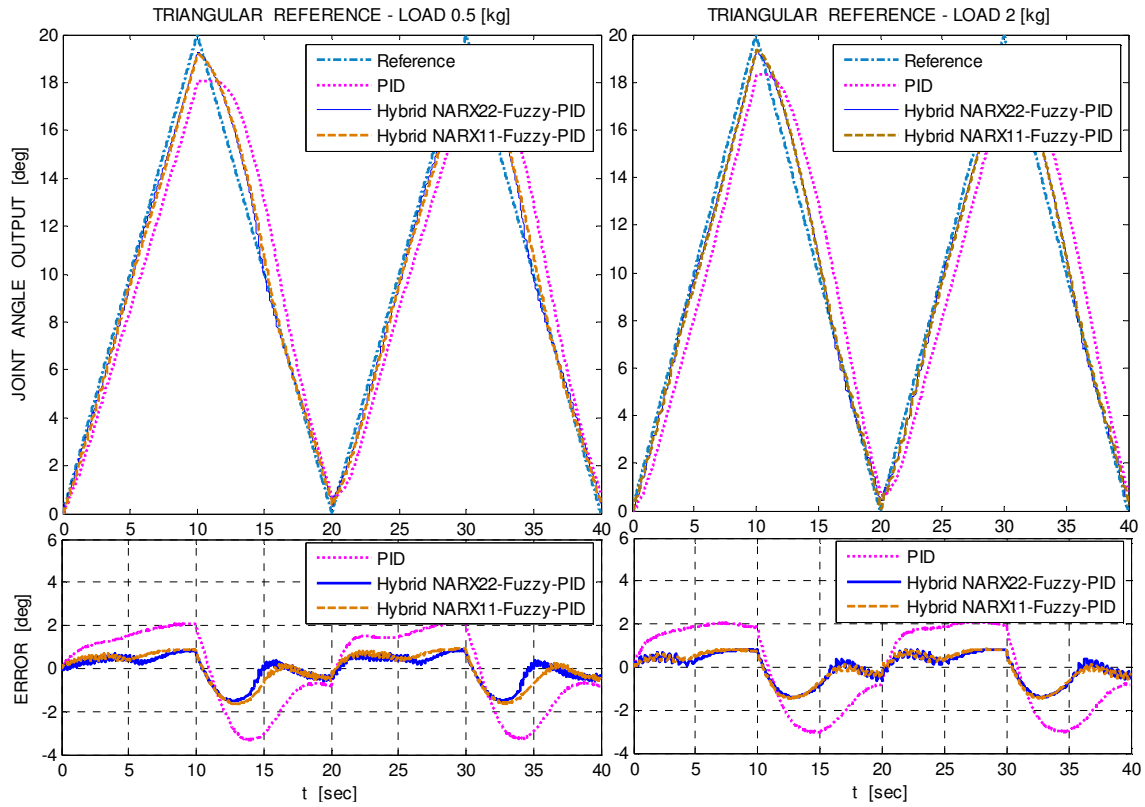

Figure 16a.Triangular response of the PAM robot arm

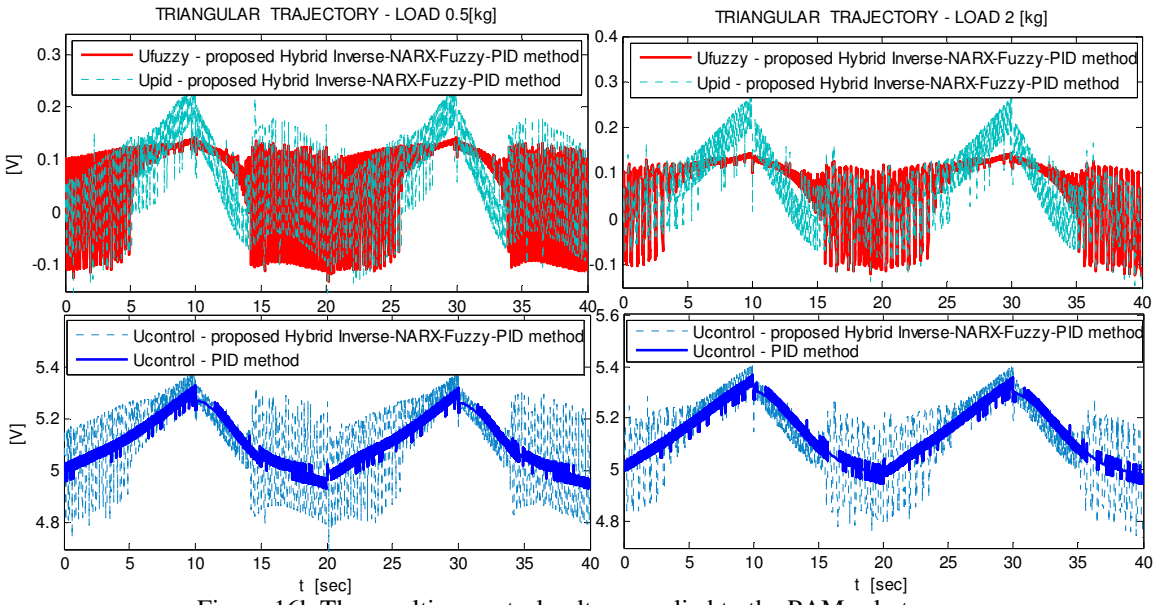

Figure 16b.The resulting control voltage applied to the PAM robot arm.

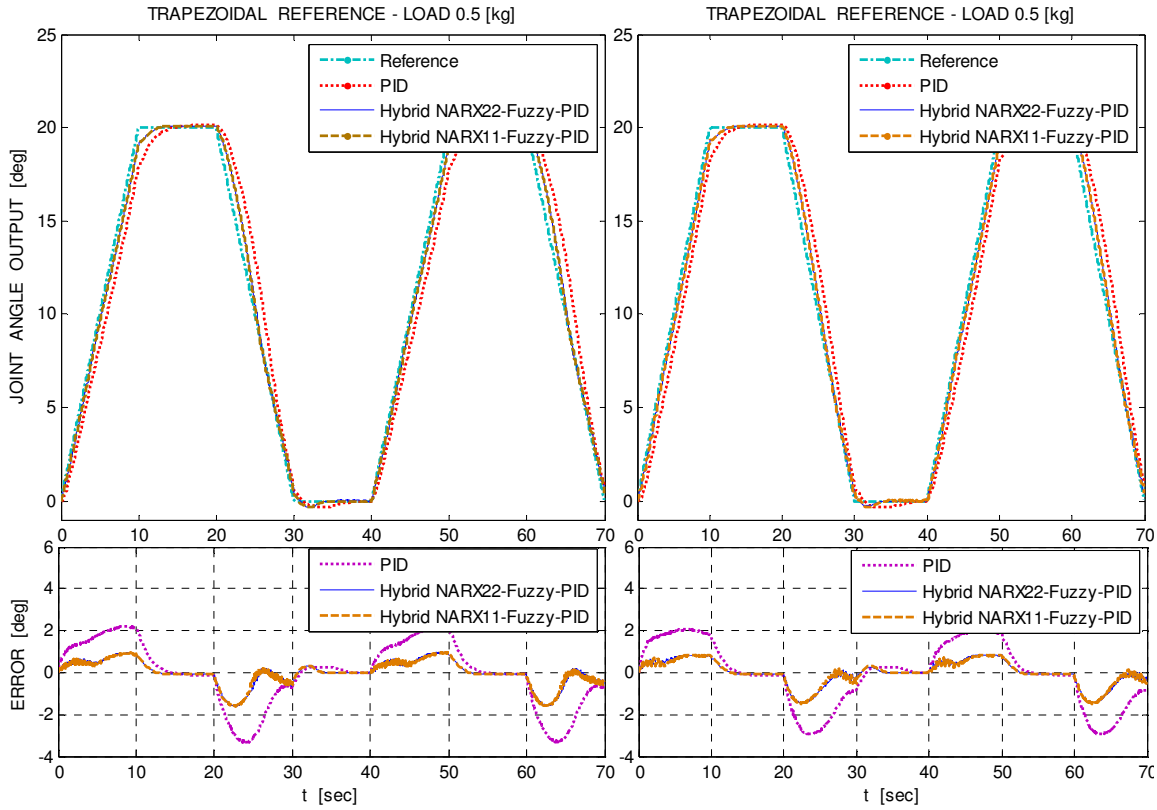

Figure 17a.Trapezoidal response of the PAM robot arm

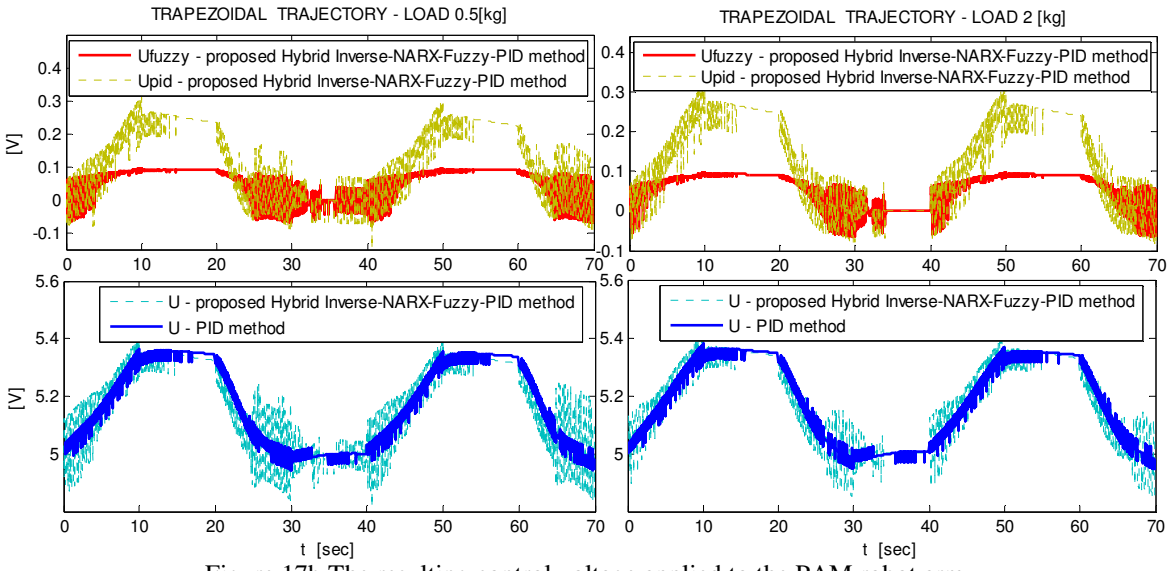

Figure 17b.The resulting control voltage applied to the PAM robot arm.

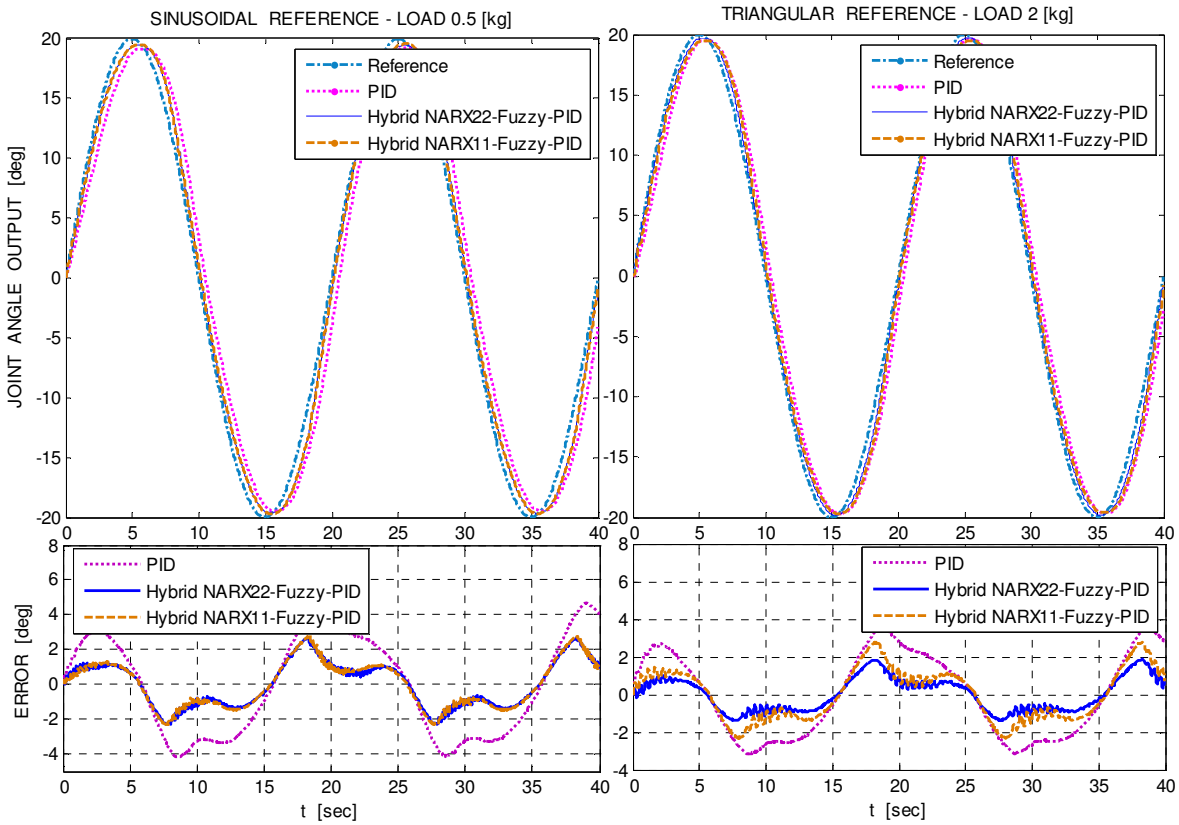

Figure 18.Sinusoidal response of the PAM robot arm

Table 1. MGA-based INFM model parameters used for encoding.

Parameter	Range	Precision	No. of Bits
Number of Membership Functions	3-5	2	1
Membership Function Spacing	0.1 – 1.0	0.1	7
Membership Function	-1 - 1	2	1
Rule-Base Scaling	0.1 – 1.0	0.01	7
Rule-Base Spacing	-1 - 1	2	1
Input Scaling	0 - 100	0.1	10
Output Scaling	0 - 1000	0.1	17
Rule-Base Angle	0 - 2π	π/512	11

Table 2. The rule-base of the MGA-based Inverse NARX11 Fuzzy Model (best fitness value = 168800)

Input2-U(z-1) / Input1-Y(z)	1	2	3	4	5
1	1	3	3	3	5
2	1	3	3	3	5
3	1	3	3	3	5
4	1	3	3	3	5
5	1	3	3	3	5

Table 3. The summary of the MGA-based PAM robot arm INFM model configuration parameters.

	Parameters	MGA-based Inverse TS Fuzzy Model	**MGA-based Inverse NARX11 Fuzzy Model**	**MGA-based Inverse NARX22 Fuzzy Model**
MGA-based Modeling Parameters	Population	20	20	20
	Generations	100	100	100
	Best Fitness Value	5807	168800	186042
Identified Inverse Fuzzy model (or Inverse NARX Fuzzy model) Configuration Parameters	Input Variables	Y and Y_{dot}	Y and U(z-1)	Y(z), Y(z-1), U(z-1) and U(z-2)
	Number of MFs of Inputs and Output	[5, 5, 9]	[5, 5, 5]	[3, 3, 3, 5, 5]
	SCALING GAIN of Inputs and Output	[98.729; 56.794; 21.057]	[2.5415; 40.567; 7.7519]	[35.973; 62.072; 30.01; 62.659; 7.9179]
	SPACING Factor of Inputs and Output MFs	[2.7609; 0.16378; 2.2359]	[0.24173; 7.7914; 3.1281]	[0.97165; 3.3509; 0.28425; 1.2815; 2.9953]
	SPACING Factor of Rule Base	[4.2617; 0.45433; 0.39055]	[3.4324; 6.3819; 1.137]	[0.97874; 0.5748; 0.41181; 1.6387; 1.0929]
	Theta Angle of rule base	[4.7331] (rad)	[1.6422] (rad)	[6.0315; 4.7208; 0.93312] (rad)
	Error Index	$> \pm$ 10[V]	$< \pm$ 0.3[V]	$< \pm$ 0.15[V]
Figures representing the results			Figures 12 and 13	Figures 14 and 15